



Measuring Apoptotic Sensitivity Through Oligonucleotide Mediated Peptide Delivery

Citation

Jung, May. 2025. Measuring Apoptotic Sensitivity Through Oligonucleotide Mediated Peptide Delivery. Bachelors Thesis, Harvard University Engineering and Applied Sciences.

Link

<https://dash.harvard.edu/handle/1/42719236>

Terms of use

This article was downloaded from Harvard University's DASH repository, and is made available under the terms and conditions applicable to Other Posted Material (LAA), as set forth at

<https://harvardwiki.atlassian.net/wiki/external/NGY5NDE4ZjgzNTc5NDQzMGIzZWZhMGFIOWI2M2EwYTg>

Accessibility

<https://accessibility.huit.harvard.edu/digital-accessibility-policy>

Share Your Story

The Harvard community has made this article openly available.
Please share how this access benefits you. [Submit a story](#)

MEASURING APOPTOTIC SENSITIVITY THROUGH OLIGONUCLEOTIDE MEDIATED
PEPTIDE DELIVERY

A thesis presented by

May Jung

to

the Faculty of the Harvard John A. Paulson School of Engineering and Applied Sciences

in partial fulfillment of the requirements for the

Bachelor of Arts degree with honors in Biomedical Engineering

Faculty Advisors: Dr. Kristopher Sarosiek and Dr. Philippe Cluzel

Postdoctoral Advisor: Dr. Zintis Inde

Harvard University

Cambridge, MA

March 28, 2025

Honor Code

In submitting this thesis to the Harvard John A. Paulson School of Engineering and Applied Sciences in partial fulfillment of the requirements for the degree with honors of Bachelor of Arts, I affirm my awareness of the standards of the Harvard College Honor Code.

Name: May Jung

Signature: 

The Harvard College Honor Code Members of the Harvard College community commit themselves to producing academic work of integrity – that is, work that adheres to the scholarly and intellectual standards of accurate attribution of sources, appropriate collection and use of data, and transparent acknowledgement of the contribution of others to their ideas, discoveries, interpretations, and conclusions. Cheating on exams or problem sets, plagiarizing or misrepresenting the ideas or language of someone else as one’s own, falsifying data, or any other instance of academic dishonesty violates the standards of our community, as well as the standards of the wider world of learning and affairs.

Acknowledgements

I would first like to thank Dr. Zintis Inde for being such an incredible advisor throughout my research journey at Harvard. The patience, compassion, and encouragement that you have shown me during these past 4 years is truly inspiring, and I am forever grateful for your mentorship. And, of course, I would not have been able to join this wonderful lab if it were not for Dr. Kristopher Sarosiek, who graciously welcomed me—a mere freshman—into some of the most interesting research endeavors. Thank you for building a genuine lab community filled with the best people. I would also like to give the biggest shoutout to the Sarosiek Lab members for always providing thoughtful advice and a helping hand (and lots of delicious snacks)!

To my advisor Dr. Philippe Cluzel, thank you for helping me structure my project and approach my research question through an engineering lens. I really appreciate you taking the time and effort to offer valuable support for my research. To Dr. Linsey Moyer, thank you for making me love my concentration. The friendships that I have made within the bioengineering community and the cherished experiences I have had as part of the teaching staff of ES 53 and as a peer concentration advisor would not have been possible without your guidance.

Lastly, I would like to thank my friends and family for making life worth living! College has truly been a long rollercoaster ride (I like rollercoasters), and I thank you for sticking by my side through the many highs and the many lows. Thank you to my dearest friends Max, Nicole, and 102 Babes for the riveting conversations, the belly laughs, and the heart-to-hearts. Thank you to my mom and dad for your sacrifices, humor, and unconditional love.

And, thank you Milky for being Milky.

Abstract

Apoptosis is a process of cell death triggered by cellular stress or extrinsic signals. In apoptosis, pro-death proteins like Bcl-2 interacting mediator of cell death (BIM) activate pore-forming proteins BAX and BAK at the mitochondria, leading to mitochondrial outer membrane permeabilization (MOMP) and downstream activation of apoptotic caspases. BH3 profiling is a method used to measure the signals required to initiate this cell death pathway. Cells are treated with peptides mimicking the Bcl-2 homology 3 (BH3) domain of pro-apoptotic proteins. By measuring responses to these peptides, BH3 profiling can compare peptide sensitivity, or “apoptotic priming,” across cell types, genotypes, or treatments. However, the requirement for membrane permeabilization limits physiological relevance and prevents longitudinal analysis. My thesis develops an alternative method for delivering BH3 peptides to living cells without membrane permeabilization. We used a trimethoprim (TMP)-inducible degron system based on a destabilized dihydrofolate reductase (DHFR) tag that enables rapid, post-translational control of protein stability. For system validation, Citrine-DHFR fusion protein was utilized, and TMP treatment induced Citrine expression in over 90% of cells at concentrations as low as 625 nM. In parallel, we optimized transfection conditions across HeLa lines with varying apoptotic sensitivity. Through *in silico* design, site-directed mutagenesis and Golden Gate cloning were used to replace Citrine with BIM and integrate the sequence into a new plasmid construct to allow future experimental validation. This system supports new extensions of BH3 profiling, including rapid nucleotide changes to expressed peptides and downstream applications such as single-cell RNA sequencing in unpermeabilized cells.

Table of Contents

<i>Honor Code</i>	2
<i>Acknowledgements</i>	3
<i>Abstract</i>	4
<i>I. Introduction</i>	8
Overview of Apoptosis	8
Apoptosis in Disease	9
Molecular Mechanisms of Apoptosis	10
Overview of Apoptotic Priming and BH3 Profiling	12
Clinical relevance of BH3 Profiling	14
Limitations of Traditional BH3 Profiling	16
Developing an Alternative BH3 Profiling Method	17
<i>II. Methodology</i>	20
Cell Culture and Maintenance	20
Preparing HeLa Cells	20
Media Preparation	20
Cell Passaging	21
Plasmid Design and Cloning	22
Plasmid Construction and Design	22
Gateway Cloning	27

Golden Gate Cloning	28
Gateway Cloning Steps.....	29
Site Directed Mutagenesis	31
Golden Gate Cloning Steps.....	32
Bacterial Culture and Plasmid Preparation.....	33
Plasmid Preparation and Dilution	33
Bacterial Culture Preparation.....	35
Bacterial Colony Transfer for Plasmid DNA.....	35
Plasmid DNA Isolation	36
Lentiviral Transduction and Selection.....	37
Transfection Setup	37
Lentiviral Infection and Selection.....	38
Bleomycin Dose-Response	38
Experimental Assays.....	39
Flow Cytometry Sample Preparation	39
Flow Cytometry Analysis	40
TMP Induction	40
BH3 Profiling.....	41
<i>III. Results</i>.....	43
Plasmid Construct.....	43
Optimization of Transfection Efficiency.....	44
Comparison of Fluorescent Protein Expression in Transfection Experiments	44

Transient Transfection Optimization	46
Apoptotic Peptide Expression with Trimethoprim.....	50
Dose-Dependent Citrine Expression.....	50
Kinetic Analysis of Apoptotic Induction.....	53
TMP Induction System	53
<i>IV. Discussion</i>	<i>54</i>
<i>V. References</i>	<i>59</i>

I. Introduction

Overview of Apoptosis

Apoptosis, the canonical form of programmed cell death, is an essential process for the normal development and homeostasis of multicellular organisms. It allows cells to self-destruct when stimulated by a trigger and is critical for processes like embryogenesis, immune system regulation, and the prevention of diseases such as cancer. Apoptosis is distinct from necrosis, which is an uncontrolled form of cell death often triggered by injury or infection. While necrosis often causes inflammation and damage to the surrounding tissue, apoptosis is a tightly regulated pathway that initiates systematic breakdown and removal of cells.

During embryogenesis, apoptosis shapes developing tissues and organs. For example, the separation of fingers and toes in humans is caused by apoptosis removing excess cells and creating appendages [1]. Apoptosis is also responsible for eliminating excess neurons during the formation of the developing brain [2]. Furthermore, the balance of cell death and proliferation in adult tissue is maintained by apoptosis. In the hematopoietic system, skin, liver, and intestines, old or damaged cells are removed, allowing for the replacement of new cells to maintain tissue homeostasis [3], [4], [5]. Apoptosis also regulates immune cells and ensures the elimination of activated immune cells or self-reactive lymphocytes. Therefore, too little apoptosis can lead to autoimmunity due to failure of proper elimination of autoreactive B-cells and T-cells, while excessive apoptosis can result in immunodeficiency. Thus, the apoptotic pathway maintains the balance in the overall immune regulation of the body [6].

Apoptosis in Disease

Apoptosis acts as a defense mechanism to eliminate cells that are harmful or damaged. Cell death is induced to prevent the spread of infection or proliferation of mutated cells to protect the organism. DNA damage in a cell will activate the G1/S check point in the cell cycle, putting it in arrest and allowing for repair before the cell begins DNA replication. If the damage is too severe, apoptosis will occur to remove the cell [7]. Cells will also undergo apoptosis in the presence of a viral infection, which will halt the production of the viral progeny [8]. Dysregulation of apoptosis plays a central role in the development of various diseases, such as cancer, neurodegenerative diseases, or autoimmune diseases.

Cancer cells often acquire mechanisms to evade apoptosis, enabling survival and proliferation despite cellular damage or abnormalities. For example, cancer cells often overexpress anti-apoptotic proteins like B-cell lymphoma 2 (BCL-2) and B-cell lymphoma-extra-large (BCL-xL). The BCL-2 family of proteins, discussed in more detail below, are named for their homology to the founding member BCL-2 and play various roles in controlling apoptosis. Overexpression of these anti-apoptotic proteins is frequently detected in many cancer cells and contributes to tumor cell survival [9]. Many cancers also upregulate proteins like X-linked inhibitor of apoptosis protein (XIAP), which directly inhibits caspases—critical effectors of apoptosis. For instance, elevated XIAP levels have been observed in pancreatic cancer, contributing to treatment resistance [10]. Apoptosis may also contribute to the loss of neurons in diseases such as Alzheimer's, Parkinson's, Amyotrophic Lateral Sclerosis (ALS), and Huntington's disease. Abnormal, misfolded protein aggregates, such as the amyloid-beta in Alzheimer's disease or alpha-synuclein in Parkinson's disease, trigger apoptotic pathways that can lead to neuronal death and pose permanent damage to the brain. Aggregated forms like

amyloid-beta interact with neural cell receptors, which can trigger caspase activation and lead to cell death [2]. Insufficient apoptosis of self-reactive lymphocytes can lead to the progression of autoimmune diseases, such as systemic lupus erythematosus (SLE) [11].

Molecular Mechanisms of Apoptosis

The pathway of apoptosis is categorized into the extrinsic pathway and the intrinsic pathway. Both pathways involve the activation of caspases, which are a family of protease enzymes that exist in their inactive proenzyme forms and are activated in response to apoptotic signals. Once the cascade is activated, critical cell structures, including the cytoskeleton and nuclear components, are broken down as the cell is prepared for efferocytosis. Efferocytosis is an anti-inflammatory process that involves the recognition, engulfment, and internalization and degradation of apoptotic cells [12].

The extrinsic pathway is also known as the “receptor mediated” pathway and is initiated by external signals that activate death receptors on the cell surface. These receptors belong to the tumor necrosis factor (TNF) receptor family. Ligands such as Fas ligand (FasL) bind to their respective death receptors and are oligomerized upon binding. The death domain of these receptors recruit the co-factor Fas-associated DD protein (FADD) for binding. Then, the death effector domain (DED) of FADD helps the complex bind to procaspase-8 [13]. This triggers the formation of the death-inducing signaling complex (DISC) [14]. DISC recruits caspase-8, an initiator caspase, which activates downstream executioner caspases like caspase-3. Caspase-3 then works to cleave actin and other substrates, leading to cell disassembly [15].

The intrinsic (mitochondrial) apoptosis pathway is activated by internal stress signals, such as DNA damage through radiation or oxidative stress. For example, stress from gamma/UV

radiation or cytotoxic drug treatment initiates signaling pathways that lead to the activation of pro-apoptotic proteins like BAX and BAK, which subsequently oligomerize to form pores on the mitochondrial outer membrane. This process triggers the release of cytochrome c, a protein normally localized in the mitochondrial intermembrane space. Once in the cytosol, cytochrome c binds to Apaf-1 (apoptotic protease-activating factor 1) and procaspase-9 to form the apoptosome, a protein complex that activates procaspase-9 into caspase-9. Caspase-9 then activates executioner caspases like caspase-3 and caspase-7, leading to cell death.

The intrinsic pathway is tightly regulated by the BCL-2 family of proteins, which control the activation of BAX and BAK. The abundance of these proteins and their binding interactions ultimately determine the fate of the cell [16]. Within the BCL-2 family, there are the anti-apoptotic proteins (BCL-2, BCL-XL, BCL-W, MCL-1 and BFL-1/A1) that prevent apoptosis by maintaining the integrity of the mitochondrial outer membrane by binding and sequestering pro-apoptotic proteins, which prevents the formation of pores in the mitochondria. This inhibits the release of cytochrome c into the cytosol, blocking the activation of downstream caspases that dismantle the cell. The pro-apoptotic proteins play the opposite role. These proteins promote apoptosis by disrupting the mitochondrial membrane through activation of the pore-forming proteins BAX and BAK.

Within the pro-apoptotic subset, two functional groups exist: activators and sensitizers [17]. Activators (BIM, BAD, BID, PUMA) directly interact with BAX and BAK and facilitate the pore formation and mitochondrial permeabilization. In contrast, “sensitizers” inhibit the anti-apoptotic BCL-2 family members but do not directly activate BAX and BAK. Ultimately, the activation of BAX and BAK commits the cell to apoptosis by inducing cytochrome c release, apoptosome formation, and caspase activation.

Both intrinsic and extrinsic apoptosis end in an execution phase, which starts with the cleavage of caspase-3 [18]. The execution phase involves key morphological changes that prepare the cell for phagocytosis. Caspases cleave proteins involved in maintaining the cytoskeleton, such as actin, gelsolin (actin binding protein), and spectrin, leading to cell shrinkage and the loss of cell shape integrity [18]. Caspases also degrade filament proteins like lamins, which are critical for the nuclear envelope's structure [19]. Degradation leads to nuclear condensation, envelope degradation, and fragmentation, and this controlled disassembly of the nucleus ensures that the cell's contents are safely packaged into apoptotic bodies— membrane bound extracellular vesicles containing cellular debris and genetic information—which are then recognized and removed, preventing the release of intracellular contents that could trigger inflammation [18], [20]. First, the cells form into a rounded morphology and detach from the extracellular matrix [21]. This is followed by the blebbing stage, where parts of the cell membrane protrude and retract to separate from the cell. Lastly, the cells condense into a small ball like shape, the cytoskeleton disassembles, and the cell fragments are phagocytosed by neighboring cells or immune cells [21].

Overview of Apoptotic Priming and BH3 Profiling

Understanding how “primed” a cancer cell is for apoptosis can help tailor cancer-targeting treatments based on a tumor's sensitivity to cell death signals. BH3 profiling is a widely-used method to measure the signals required to initiate apoptosis [17]. BH3 profiling was developed as a tool to functionally assess how “primed” a cell is to undergo apoptosis. Instead of measuring individual protein levels or interactions, BH3 profiling tests how the mitochondria of permeabilized cells responds to synthetic peptides derived from the BCL-2 homology (BH3)

domain of pro-apoptotic proteins. BIM and BID BH3 peptides bind to anti-apoptotic proteins or bind and activate pro-apoptotic pore-forming proteins BAX and BAK [22]. The PUMA2A peptide, often used as a control, can bind to the pro-apoptotic proteins but cannot activate them. The cellular response caused by the treatment of these peptides reveals how sensitive a cell is to apoptotic stimuli. The BH3 profiling assay typically follows four main steps [22]. Cells are gently permeabilized with low concentrations of digitonin and are simultaneously treated with titrated doses of pro-apoptotic BH3 peptides. In cells that are primed to undergo apoptosis, this peptide treatment will cause MOMP, which will release cytochrome c into the cytosol. Lastly, a staining dye is used to measure the loss of cytochrome c in cells.

To understand apoptotic priming, the “cliff model” is commonly used [23]. Cells that are closer to the edge of the cliff means that they are more primed for apoptosis and will “fall off the cliff” more easily, meaning they undergo cell death more readily when exposed to stress or therapeutic agents. The analogy represents how easily a cell can be “pushed” into apoptosis: cells on the edge of the cliff are more sensitive, while those further back are more resistant. This model can be understood with two main categories: “primed” and “unprimed” [24]. Primed cells are highly sensitive to apoptosis, or “primed for death”, meaning they are close to the cliff’s edge, and even minimal stress or signaling can trigger apoptosis. Unprimed cells have intact downstream apoptotic machinery, including functional BAX and BAK proteins. However, the upstream activation of BH3 proteins is inhibited, making them less likely to be activated by pro-death signals and keeping them at a safer distance from the cliff’s edge. Some cells entirely lack functional BAX and BAK effector proteins due to mutations or insufficient expression. These cells are resistant to apoptosis via the intrinsic pathway, as they lack the necessary machinery to execute apoptosis.

Clinical relevance of BH3 Profiling

BH3 profiling has significant clinical implications, especially in cancer treatment. While some cancers evade apoptosis by upregulating anti-apoptotic proteins, cancer cells are often more primed for apoptosis than the normal tissue from which they arise. This difference in priming is what allows chemotherapy to selectively target cancer cells—by administering a broadly toxic drug, the goal is to push primed cancer cells past the apoptotic threshold while sparing the less primed cells. BH3 profiling helps to identify which anti-apoptotic proteins are active in cancer cells. It uses BH3 peptides to bind and neutralize specific anti-apoptotic proteins, leading to MOMP and providing insights for targeted therapies that inhibit these anti-apoptotic proteins.

For example, ABT-199 (Venetoclax) is a selective inhibitor that specifically targets BCL-2 and is effective in cancers that are dependent on the anti-apoptotic protein BCL-2 for survival, like chronic lymphocytic leukemia (CLL) [25], [26]. High levels of BCL2 in CLL cells create a dependency on this protein for survival, which also makes the cells vulnerable to BCL2 inhibitors like venetoclax. Patient studies have demonstrated a strong correlation between mitochondrial priming, as assessed by BH3 priming, and treatment outcomes with venetoclax [26]. Patients with CLL cells exhibiting high levels of mitochondrial priming showed lower level of lymphocytes. Reduced lymphocyte levels reflect rapid induction of apoptosis in CLL cells, indicating effective treatment and thus a favorable therapeutic response. By targeting BCL2, venetoclax disrupts the survival mechanism of primed CLL cells, ultimately reducing lymphocyte counts and improving clinical outcomes.

BH3 profiling can simulate the effects of venetoclax on the mitochondria, and this relationship underscores the potential of BH3 profiling to not only act as a biomarker for drug

response but also a tool in identifying patients that are most likely to benefit from BCL-2 target treatments, which further personalizes the treatment process. Furthermore, BH3 profiling also helps us understand a cell's sensitivity to chemotherapy and identify cells that are more primed and thus more likely to respond to the treatment. When using existing techniques that only measure protein expression levels (e.g., Western Blotting), it's difficult to account for cells that have a high level of the pro-apoptotic BAX protein that is inactive or sequestered by the anti-apoptotic proteins like BCL-2. The presence of BAX alone does not directly correlate to the cell undergoing apoptosis. The cells will only undergo apoptosis if BAX creates pores in the mitochondrial membrane and allows for the release of cytochrome c into the cytosol. BH3 profiling provides a functional readout and directly tests how these proteins are interacting inside the cell.

It's important to note that two key measurements are assessed using BH3 profiling: apoptotic "sensitivity" and "dependency". Apoptotic sensitivity is gauged by using activator peptides, such as BIM or BID, which reveals how much stimulus is needed to induce MOMP and initiate apoptosis. These peptides mimic pro-apoptotic proteins by directly activating BAX and BAK. Thus, highly sensitive cells (primed for apoptosis) require only a small amount of activator peptides to trigger apoptosis, while less sensitive cells (unprimed) need much more peptide to achieve the same response. With apoptotic dependency, BH3 profiling uses sensitizer BH3 peptides, such as BAD and NOXA, which do not directly activate BAX and BAK but instead bind to and inhibit pro-survival proteins. For example, the BAD peptide binds to BCL-2 and BCL-xL, while NOXA binds to MCL-1. Adding these sensitizer peptides to permeabilized cells allows us to identify which pro-survival proteins the cells rely on for survival.

Limitations of Traditional BH3 Profiling

Although BH3 profiling, as forementioned, is a widely used technique, it requires permeabilizing the cell membrane, which poses certain limitations. Permeabilization can lead to changes in the cell's internal environment, which brings upon the issue of not being able to fully display the cell's behavior under physiological conditions. For cells that are sensitive, permeabilization can induce unintended changes in the cytoplasmic protein levels or disrupt protein-protein interactions. This can disturb the interpretation of results, as it becomes challenging to distinguish between what is caused by apoptotic priming and what is caused by the permeabilization. Another key limitation of permeabilization is the inability to perform certain downstream analyses. For example, RNA sequencing is a powerful tool for studying which specific genes are active in cells and, thus, reveals how cells respond to different conditions and what genes may influence their behavior. However, permeabilizing the cell membrane can cause the cell's contents to leak out, which can lead to RNA degradation, making it difficult to perform high-quality RNA sequencing.

Additionally, membrane permeabilization can affect the cell's ability to be used in longitudinal studies. Cells cannot be kept alive for extended periods of time, so researchers can only obtain a snapshot of apoptotic priming at a single point in time. This prevents monitoring dynamic changes within the cell in response to other stimuli or treatments. Temporal studies, such as understanding how cells may adapt to stress over time or how their apoptotic threshold may be affected in response to environmental changes or therapeutic treatments, are particularly made difficult with the limitation posed by traditional BH3 profiling methods. Therefore, there is a need for an alternative approach that avoids membrane permeabilization.

Developing an Alternative BH3 Profiling Method

Gao et al.'s 2018 paper *Programmable Protein Circuits in Living Cells* describes the use of viral proteases to create modular, programmable protein circuits within cells. Their approach leverages proteases that interact with target sites on other proteins to precisely regulate protein interactions and cellular responses [27]. My proposed study builds upon the research of Gao et al. to develop an alternative approach for delivering pro-apoptotic stimuli in cells without the need for plasma membrane permeabilization. Gao et al. demonstrated a degron-based system with engineered protein circuits capable of controlling protein activity through precise proteolytic cleavage. Inspired by this approach, I hypothesize that using an oligonucleotide-mediated BH3 profiling approach for pro-death stimuli delivery, which eliminates the need for membrane permeabilization, will yield more accurate measurements of apoptotic priming and allow for additional downstream analyses.

Gao et al. utilizes the DHFR degron system, which is based on fusing a protein of interest—in this case the fluorescent protein Citrine—to a destabilizing domain, a modified dihydrofolate reductase (DHFR). Under normal conditions, the DHFR domain is rapidly targeted for ubiquitination and rapid proteasomal degradation. Proteins marked with ubiquitin tags are recognized and broken down into short peptides by the proteasome [28]. However, the addition of the antibiotic trimethoprim (TMP), a ligand with high affinity for DHFR, stabilizes the DHFR domain by binding to its active site [29]. This conformational stabilization blocks the recognition required for ubiquitination and halts the degradation process. The stabilized Citrine-DHFR fusion protein can then accumulate and function within the cell. TMP can effectively “turn on” protein stability, which offers a faster response when compared to traditional transcriptional induction systems.

For example, in doxycycline-based inducible systems, gene expression is regulated at the transcriptional level. Adding the antibiotic doxycycline starts transcription of the target gene, but this takes time as the cell has to go through transcription and translation to produce the protein [30]. In contrast, the DHFR degron system with TMP works directly on the protein that is already made. TMP stabilizes the DHFR-tagged protein instantly by stopping the degradation process. Beyond the TMP system, Gao et al. also demonstrated a protease dependent system, specifically Tobacco Etch Virus Protease (TEVP) and Tobacco Vein Mottling Virus Protease (TVMVP). By embedding cleavage sites for TEVP or TVMVP in the Citrine-DHFR construct, researchers can selectively control when a protein is activated or inactivated. When TEVP or TVMVP cleaves the site on the target protein, it removes the destabilizing domain, which allows the citrine fluorescent tag to be expressed and detected.

Gao et al.'s experimental setup offers a foundation for developing an oligonucleotide-based BH3 profiling method. For this study, instead of Citrine, BH3 peptides are encoded by oligonucleotides and fused to the DHFR degron tag. Under normal conditions, the DHFR degron ensures rapid degradation of the BH3 peptides, preventing them from triggering apoptosis. Upon adding TMP, the DHFR degradation pathway would be inhibited, stabilizing the BH3-DHFR fusion peptide. This allows BH3 peptides to accumulate in the cell, where they could interact with the BCL-2 family proteins and initiate apoptosis in primed cells. This setup provides temporal control, meaning we can decide when the BH3 peptide is stabilized and when it can interact with its targets. Incorporating TEVP and TVMVP cleavage sites offer another layer of control. For example, even if the BH3 peptide is stabilized with TMP, cleavage of TEVP or TVMVP can be used to activate the fusion protein under certain conditions, which offers another switch mechanism for activating or inactivating the peptide. The BH3-DHFR protein can be

designed so that applying TMP prevents protein degradation and cleaving the DHFR tag activates the BH3 peptide. Together, the system gives precise control over when and where the BH3 peptide is active to improve the flexibility and efficiency of BH3 profiling.

In this study, using a TMP-inducible DHFR degron system, I demonstrated that TMP-mediated stabilization effectively regulates protein expression. This provided a controllable system for delivering pro-apoptotic peptides. Flow cytometry analysis confirmed that TMP addition led to a dose-dependent increase in Citrine fluorescence, validating the system's ability to regulate protein stability. In parallel, I successfully completed the in-silico design and cloning strategy for the BH3-DHFR fusion construct, including the incorporation of necessary restriction sites for downstream plasmid assembly.

II. Methodology

Cell Culture and Maintenance

Preparing HeLa Cells

HeLa cell lines were utilized in this study, including wildtype (WT), BAX knockout (KO), BAK knockout, and double knockout (DKO). WT cells express functional BAX and BAK, while DKO cells, lacking both, serve as a model for high apoptotic resistance. The KO and DKO cell lines were previously generated using the CRISPR-Cas9 gene-editing system [31]. Two guide RNAs were designed to specifically target the BAX and BAK genes. The CRISPR-Cas9 system introduced small cuts in the DNA at these locations, forming double-strand breaks. These were then repaired through the cell's non-homologous end joining repair mechanism. This process leads to insertion and deletion mutations in the target exons, generating a premature termination codon in the mRNA. These mutations effectively turn off the BAK and BAX genes.

Media Preparation

Dulbecco's Modified Eagle Medium (DMEM) was warmed in a water bath and combined with 50 mL of fetal bovine serum (FBS) and 5 mL of Penicillin-Streptomycin (P/S) to a total volume of 500 mL. The solution was sterile filtered using a 500 mL vacuum flask. The prepared media was then stored at 4° C and warmed to 37° C for use.

Cell Passaging

- **Suspension Cells:** To prepare a new batch of cells, 25 mL of complete media was first transferred into a new flask. Approximately 1.5 million cells were added. For cell counting, 750 μ L from the old flask was pipetted into a 4 mL tube for analysis. Cells were counted by Beckman Coulter Vi-Cell, which measures viability by Trypan Blue staining. After assessing viability, the cells in media were transferred into the new flask, adjusting the volume according to cell concentration. The new flask was then placed in the incubator.
- **Adherent Cells:** Cell density was checked under a microscope. 25 mL of fresh media was added to a new flask. The old media was removed using a vacuum, and 5 mL of Hank's Balanced Salt Solution (HBSS) was used to rinse the cells. Direct pipetting on the cells was avoided. HBSS was removed, 1.5 mL of trypsin was added to the flask, and the flask was tilted to ensure even coverage of cells with trypsin. The flask was placed in the incubator for five minutes. Complete trypsinization was confirmed via the observation of floating and rounded cells under a microscope. To halt trypsin digestion, 3.5 mL of media was added. The suspension was pipetted up and down to ensure an even single-cell distribution. A sample of 750 μ L was taken for cell counting. Based on the count, the appropriate volume of viable cells was transferred into the new flask. The new flask was placed in the incubator. The remaining cells were properly disposed of, and the hood and workspace were cleaned thoroughly with 70% ethanol to prevent contamination.
- Cells were split according to the following schedule
 - o 1-day split: seeded 3 million cells
 - o 2-day split: seeded 1.5 million cells

- 3-day split: seeded 750,00 cells
- 4-day split: seeded 375,000 cells

Plasmid Design and Cloning

Plasmid Construction and Design

The plasmid design was performed using SnapGene, a molecular biology software that allows for in silico cloning, site-directed mutagenesis (SDM), and sequence visualization. The goal was to construct plasmids for inducible BIM expression, control of expression/degradation by proteases, and fluorescent reporters, ensuring their correct integration into lentiviral (PLX) or piggyback transposase-based (PB-PGK) vectors. The process involved designing primers, inserting mutations, simulating restriction cloning, performing in silico Gateway Cloning, and verifying sequences before experimental validation.

The pDONR221 plasmid is an entry vector used in Gateway Cloning to facilitate the transfer of genes into different destination vectors (pCW57.1 and pLX_TRC311). It acts as an intermediate plasmid that temporarily houses BIM, TEVP, and TVMVP before their final insertion into pcw57.1 or PLX during the LR reaction. Both pCW57.1 and pLX_TRC311 contain sequence elements for lentiviral packaging, enabling stable integration into the genome. However, their key difference lies in their promoters. pCW57.1 contains an inducible tetracycline response element TRE promoter, allowing doxycycline-regulated gene expression. On the other hand, pLX_TRC311 contains a constitutive promoter, leading to continuous gene expression.

1. Creating a New Plasmid File and Importing Sequences

- a. To begin the plasmid design, the sequences of the backbone vector (PB-PGK-Citrine-TEVS-DHFR, pDONR221, or pcw57.1) and gene inserts (BIM, TEVP, TVMVP, or Citrine) were imported into SnapGene from Addgene, a plasmid repository.
- b. Once the sequence was in SnapGene, it was converted into a circular plasmid map, allowing for visualization of key features such as promoters, antibiotic resistance genes, and recombination sites.
- c. When designing pENTR BIM, the BIM gene sequence was inserted into pDONR221, ensuring the presence of attL recombination sites for subsequent Gateway cloning. For Golden Gate Cloning, the BIM sequence was modified to include BsaI restriction sites and overhangs compatible with the Golden Gate backbone.

2. Primer Design for PCR and Mutagenesis

- a. With the base plasmid established, primers were designed for PCR amplification of inserts and site-directed mutagenesis. SnapGene's "Create Primers" tool was used to design forward and reverse primers that flanked the regions of interest.
- b. Gateway Cloning (attB Primers): For Gateway Cloning, primers were designed to introduce attB recombination sites flanking the BIM, TEVP, and TVMVP genes. In SnapGene, the BIM gene sequence was selected, and the attB site sequences were manually added to the 5' and 3' ends. The Primer Design tool was used to generate high-specificity primers, ensuring optimal melting temperature (T_m) for

PCR. The final primers were exported as a primer list and ordered for PCR amplification.

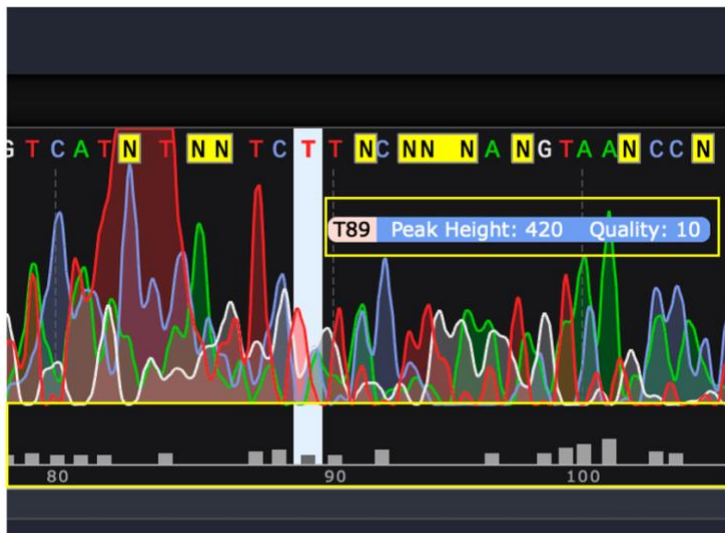
- c. Site-Directed Mutagenesis (SDM): For mutagenesis of the PB-PGK-Citrine-TEVS-DHFR plasmid, three mutation sites were introduced at 7016, 4569, and 1919 base pair locations to accommodate Golden Gate Cloning. Specifically, the goal was to add BsaI restriction sites flanking the Citrine sequence while removing any other BsaI restriction sites in the plasmid to prevent unwanted restriction digestion during the cloning process. The "Mutagenesis" tool in SnapGene was used to introduce point mutations by selecting the target base pair position and specifying the desired base substitution. At each sites a point mutation was introduced to prevent unwanted restriction digestion. NEBaseChanger, a web-based tool to design primers for SDM experiments, generated forward and reverse primers for each mutation, ensuring that the primer T_m matched the optimal annealing conditions.
 - d. Golden Gate Cloning (BsaI Primers): To insert BIM into the PB-PGK-Citrine-TEVS-DHFR plasmid, BsaI restriction sites were added using custom primers. The fragment containing BIM was selected, and BsaI recognition sites were added using the SnapGene Golden Gate Assembly Function.
3. Simulating In Silico Cloning
- a. Before performing experimental cloning, SnapGene was used to simulate the cloning process, ensuring that all modifications would work as intended.
 - b. Simulating BP and LR Gateway Cloning: For Gateway Cloning (details further explained in a later section), SnapGene's "BP Reaction" and "LR Reaction" tools

were used to simulate the insertion of attB-flanked BIM into pDONR221, creating pENTR BIM, and subsequently transferring it into pcw57.1 or PLX. The software automatically recognized attB/attP recombination sites and displayed the resulting attL/attR junctions in the final constructs. This step ensured that the reading frame was maintained, preventing frameshift mutations in the expressed protein.

- c. Simulating Golden Gate Assembly: For Golden Gate Cloning, SnapGene simulated the ligation of BsaI-digested BIM into PB-PGK-Citrine-TEVS-DHFR. The vector and insert were both virtually digested with BsaI to confirm correct fragment sizes. The software checked for correct overhang sequences to ensure precise recombination.
4. Sequence Verification and Annotation: After constructing the virtual plasmids, SnapGene's "Auto-annotate" function was used to verify key features. Promoters, resistance genes, restriction sites, and recombination sequences were annotated for quick reference. SnapGene's "Align Sequences" tool was used to compare the designed plasmid with reference sequences from Addgene. Each construct was exported as a FASTA file for comparison with sequencing data after experimental cloning. For example, after performing BP and LR reactions, the pENTR BIM and PLX-BIM plasmids were sequenced. The Sanger sequencing results were aligned in SnapGene, confirming the correct integration of BIM.



3-mPGK-F



4-mPGK-F

Figure 1: Sequencing reads through SnapGene. The top panel shows a high-quality sequencing read (A89, peak height 1372, quality score 59), while the bottom panel displays a low-quality read (T89, peak height 420, quality score 10). The low-quality read suggests sequencing artifacts or poor template quality.

5. **Generating Final Expression Constructs:** The final constructs were optimized for mammalian expression, ensuring compatibility with inducible expression systems (TMP, doxycycline) and lentiviral packaging. For doxycycline-inducible BIM expression, the final pcw57.1-BIM plasmid was designed with the TRE promoter upstream of BIM. For lentiviral packaging, the PLX-BIM plasmid already contains long terminal repeats (LTRs) for stable genomic integration. However, constitutive BIM expression was avoided due to its potential to induce cell death. Instead, the focus was on inducible systems to tightly regulate BIM expression. For protease-based degradation assays, the PB-PGK-Citrine-TEVS-DHFR plasmid was mutated to allow for TEVP-dependent cleavage. Once validated, the lentiviral plasmids were transfected into HEK293T, human embryonic kidney cells, to produce lentiviral particles, which were then used to infect HeLa cells for downstream experiments.

Gateway Cloning

This method is a site-specific recombination system that enables the seamless transfer of genes between vectors without the need for restriction enzymes or ligases. The system relies on four distinct recombination sites—attB, attP, attL, and attR—to facilitate gene transfer through two sequential reactions: the BP reaction and the LR reaction.

- The BP reaction is the first step in Gateway Cloning and is responsible for generating an entry clone, which serves as an intermediate vector that temporarily houses the gene before it is transferred into the final expression vector. In this reaction, the attB sites flanking the gene of interest recombine with the attP sites present in the pDONR221 vector. This recombination is catalyzed by BP Clonase, an enzyme mixture that facilitates the exchange of DNA sequences. As a result, the attB and attP sites are converted into

attL sites, creating a recombinant plasmid known as pENTR_Citrine_tevs_DHFR. This plasmid contains the citrine fluorescent protein used as a reporter, the TEV (Tobacco Etch Virus) protease cleavage site, which allows controlled removal of the degon, and the DHFR (Dihydrofolate Reductase) degon, which enables TMP-dependent protein stabilization.

- Once the entry clone has been validated, the LR reaction is performed to generate the final expression construct. In this step, the attL sites in the pENTR plasmid recombine with the attR sites present in the destination vector (pCW57.1 or pLX_TRC311). A destination vector is the plasmid that carries the necessary elements for gene expression, such as a promoter and selection marker. This recombination, catalyzed by LR Clonase, transfers the gene into the expression vector while simultaneously converting attL and attR sites back into attB and attP sites. This ensures that the recombination process is reversible and modular, allowing for efficient transfer of multiple genes between different vectors without additional restriction enzyme digestion.

Golden Gate Cloning

Golden Gate Cloning relies on the ability of type IIS restriction enzymes to generate overhangs that facilitate precise fragment assembly in a predetermined order. Both BsaI and BbsI are type IIS restriction enzymes that recognize specific DNA sequences but cut at a distance away from their recognition sites. This feature makes them valuable tools in Golden Gate Cloning, as they enable seamless DNA assembly without introducing extra base pairs or restriction site scars.

We considered cloning strategies relying on either BbsI or BsaI. While both BbsI and BsaI could have been used, the use of BbsI would have required four separate site-directed mutagenesis steps to eliminate or reposition recognition sites that interfered with cloning. In contrast, BsaI required only three SDM steps, making it more efficient.

To confirm the feasibility of using BsaI, we performed an *in silico* digest—a computer simulated restriction enzyme digestion using SnapGene. This analysis allowed us to visualize how BsaI sites would be processed within the PB-PGK-backbone and BIM insert. The *in silico* digest confirmed that BsaI generated the correct overhangs required for efficient ligation and assembly into the final construct.

Gateway Cloning Steps

- **BP Reaction (Generating Entry Clones):** The BP reaction was performed to insert BIM, TEVP, and TVMVP genes into pDONR221, creating the entry clones pENTR BIM, pENTR TEVP, and pENTR TVMVP. To ensure proper dilution, the PCR product was adjusted to a final concentration of 10 ng/μL before use. For highly concentrated samples (e.g., 1000 ng/μL), a 1:50 dilution was prepared by mixing 2 μL of PCR product with 98 μL of TE buffer, achieving a 20 ng/μL concentration. This allowed for precise volume adjustments before proceeding with recombination. The BP reaction mix was assembled in a 1.5 mL microcentrifuge tube, containing 2 μL of attB-PCR product (10 ng/μL), 1 μL of pDONR221 plasmid (150 ng/μL), and 5 μL of TE Buffer (pH 9), totaling 8 μL. The BP Clonase II enzyme mix was thawed on ice for 2 minutes, vortexed briefly twice, and 2 μL was added to the reaction mix. The reaction was vortexed again, centrifuged, and incubated at 25°C for 1 hour. Following incubation, 1 μL of Proteinase

K solution was added to terminate the reaction, followed by a 10-minute incubation at 37°C. To ensure correct recombination, ccdB selection was employed. The pDONR221 vector contains the ccdB gene, which is toxic to standard E. coli strains. During a successful BP reaction, the ccdB gene is replaced by the gene of interest, allowing only correctly recombined plasmids to survive. If recombination fails, the ccdB gene remains intact, leading to bacterial cell death upon transformation. The BP reaction products were transformed into NEB 10-beta competent bacteria, which are ccdB-sensitive, ensuring selection of only successfully recombined plasmids. Transformed bacteria were plated on kanamycin-containing LB agar plates and incubated at 37°C overnight. Colonies were picked and transferred into liquid TB media with kanamycin for further propagation. Plasmids were extracted using a miniprep procedure, and sequencing was performed to confirm proper BIM insertion into pDONR221.

- **LR Reactions (Generating Expression Clones):** Following successful BP recombination and sequencing validation, the LR reaction was performed to transfer BIM, TEVP, and TVMVP genes into their respective destination vectors. The BIM gene was transferred into pcw57.1, generating pcw57.1-BIM, while TEVP and TVMVP were cloned into PLX. The LR reaction was set up in a 1.5 mL microcentrifuge tube, containing 3 µL of TEVP (36.9 ng/µL), 8 µL of PLX (35.3 ng/µL), 4 µL of 5X LR Clonase Reaction Buffer, and 1 µL of TE Buffer (pH 8), bringing the total reaction volume to 16 µL. The LR Clonase enzyme mix was thawed on ice, vortexed briefly twice, and 4 µL was added to each reaction tube. The reaction was centrifuged and incubated at 25°C for 1 hour. Following incubation, 2 µL of Proteinase K solution was added to terminate the reaction, followed by a 10-minute incubation at 37°C. The

transformation process for LR reaction products mirrored the BP reaction, with transformed NEB 10-beta competent bacteria plated onto ampicillin-containing LB agar plates instead of kanamycin plates. Successfully recombined clones were verified by sequencing, ensuring the correct positioning of BIM downstream of the TRE promoter in pcw57.1 and TEVP/TVMVP in PLX.

Site Directed Mutagenesis

To introduce specific mutations into the PB-PGK-Citrine-TEVS-DHFR plasmid, a Q5 Site-Directed Mutagenesis approach was used. For Golden Gate Cloning in later steps, the PB-PGK-Citrine-TEVS-DHFR plasmid required modifications via SDM. This was necessary to introduce specific restriction sites for precise DNA assembly. To ensure compatibility with BsaI digestion, SDM was performed to remove unintended BsaI sites while retaining recognition sequences flanking the BIM insert.

The reaction components included Q5 Hot Start High-Fidelity 2X Master Mix (12.5 μ L), 10 μ M Forward and Reverse Primers (1.25 μ L each), Template DNA (1 μ L at a concentration of 1–25 ng/ μ L), and 9.0 μ L of nuclease-free water, making up a total reaction volume of 25 μ L. The reaction was thoroughly mixed before being placed in a thermocycler for exponential amplification.

Thermal cycling conditions consisted of an initial denaturation step at 98°C for 30 seconds, followed by 25 cycles of denaturation at 98°C for 10 seconds, annealing at 70°C for 20 seconds, and extension at 72°C for 25 seconds per kilobase. A final extension at 72°C for two minutes completed the reaction. This was followed by a hold at 4°C. The specific annealing

temperatures varied based on primer design, with 70°C used for the mutation at site 7106, requiring a total extension time of 3 minutes and 15 seconds for a 7.8 kb plasmid.

Following PCR amplification, the KLD (Kinase, Ligase, and DpnI) reaction was performed to remove the parental plasmid and circularize the newly mutated plasmid. The PCR product (1 µL) was combined with 5 µL of 2X KLD Reaction Buffer, 1 µL of 10X KLD Enzyme Mix, and 3 µL of nuclease-free water, making up a total volume of 10 µL. The reaction mixture was incubated at room temperature for 5 minutes.

To introduce the mutated plasmid into bacteria, a heat-shock transformation was performed using NEB 5-alpha Competent *E. coli* cells (C2987 strain). The competent cells were thawed on ice, and 5 µL of the KLD mix was added to 50 µL of cells. The cells were mixed gently and incubated on ice for 30 minutes, followed by heat shock at 42°C for 30 seconds and immediate incubation on ice for 5 minutes. Next, 950 µL of SOC media was added, and the cells were incubated at 37°C for 60 minutes with shaking (250 rpm). After incubation, 50–100 µL of the transformation mix was spread onto carbenicillin-containing LB agar plates and incubated overnight at 37°C.

Golden Gate Cloning Steps

The primer design process was carried out using NEBaseChanger. The flanking regions of the BIM insertion site were selected and modified to include BsaI restriction sites. Specific mutations were introduced at position 3402 (A→G substitution) to accommodate restriction digestion, as well as at positions 1926–1927 (GT→AT) and 2670–2576 (GAAGAC multiple substitution) to ensure proper enzyme recognition and overhang compatibility. Following sequence modifications, the entire plasmid was amplified using PCR. The PCR-amplified

plasmid was then analyzed and verified through sequence alignment, confirming that all restriction site modifications were correctly incorporated.

Bacterial Culture and Plasmid Preparation

Plasmid Preparation and Dilution

Plasmids were prepared and quantified for bacterial culture and lentiviral transduction. These DNA constructs were diluted to optimal concentrations before transformation into competent bacteria. The key plasmids included the Citrine-DHFR expression vector and packaging plasmids. Plasmid DNA concentration was measured using a NanoDrop spectrophotometer. A 1 μL drop of water was first used to calibrate the device, followed by a 1 μL drop of plasmid DNA sample. For plasmid verification, both Sanger sequencing and whole-plasmid sequencing were used:

- Sanger sequencing was a targeted approach used to validate key insertion sites. Primers were designed to sequence across attL/attR recombination sites in Gateway Cloning constructs and confirm proper integration of gene inserts.
- Whole plasmid sequencing was conducted to verify full plasmids, especially for constructs with multiple modifications. This method provided a complete sequence readout to detect errors such as unwanted mutations or recombination artifacts.

To prepare plasmids for Sanger sequencing, samples were diluted to below 50 ng/ μL using water. Samples with less than 25 ng/ μL were disregarded. Five microliters of each diluted plasmid DNA sample was transferred into small strip tubes and sent for sequencing.

Plasmid Name	Addgene Catalog #	Bacterial Resistance Marker
pCMV-VSV-G	8454	Ampicillin
pMDLg/pRRE	12251	Ampicillin
pRSV-Rev	12253	Ampicillin
PGK-H2BmCherry	21217	Ampicillin
pCMV-Tag2B Flag BimEL	23090	Kanamycin
pCMV-Tag2B Flag BimS	23283	Kanamycin
pCW57.1	41393	Chloramphenicol and Ampicillin
pLX_TRC311	113668	Chloramphenicol and Ampicillin
PB-PGK-Cit-tevs-DHFR	116040	Ampicillin
PB-PGK-teD-Cit	116041	Ampicillin
PB-PGK-Cit-tvmvs-DHFR	116042	Ampicillin
PB-PGK-tvD-Cit	116043	Ampicillin
CMV-TO-TEVP	116062	Ampicillin
CMV-TO-TVMVP	116078	Ampicillin
pDONR221	NA	Kanamycin
pENTR_Citrine-tevs-DHFR	NA	Ampicillin
PB-PGK-BIMS-tevs-DHFR	NA	Ampicillin
pLX_TRC311_Citrine-tevs-DHFR	NA	Chloramphenicol and Ampicillin

Figure 2: List of plasmid constructs. The table includes necessary information on all plasmids used in the study, including name, catalog number on Addgene, and bacterial resistance marker.

Bacterial Culture Preparation

Plasmid DNA was obtained from Addgene as bacterial stabs, which were received as pre-transformed glycerol stock in *E. coli*. These stocks were used to inoculate agar plates for plasmid amplification. To prepare cultures for plasmid DNA extraction, bacterial stabs were streaked onto antibiotic agar plates, allowing colony formation. Agar plates were made using Terrific Broth (TB) media and ampicillin to grow bacteria. For the bacterial culture, 14.28 g of TB, 1.2 mL of glycerol, and 9.6 g of Luria-Bertani agar were used to create the plate mixture. A 5 mL pipette was used to add glycerol. The prepared mixture was sterilized using an autoclave. After sterilization and partial cooling, 300 μ L of the appropriate antibiotics (either carbenicillin or kanamycin, depending on the plasmid selection marker) was added to the mixture. Carbenicillin was used to select bacteria with plasmids that were ampicillin resistant. Finally, the sterile medium was poured into petri dishes and allowed to solidify, creating the TB plates used for bacterial growth. Once the plates were prepared, bacterial colonies were streaked onto the antibiotic-containing medium to select for successfully transformed bacteria. These colonies were incubated overnight at 25°C before being used for plasmid DNA extraction.

Bacterial Colony Transfer for Plasmid DNA

After bacterial growth on the agar plates was confirmed, liquid cultures were prepared for plasmid DNA extraction. For this step, bacterial cultures were grown in liquid media. Each tube contained 2 mL of TB mixed with 10 μ L of ampicillin from a 10 mg/mL stock, making a final concentration of 100 μ g/mL. Each individual culture was inoculated by selecting a single

bacterial colony from a plate using a sterile pipette tip and depositing the tip into the prepared tube. If the colony plate appeared too dense, a restreak was performed to isolate distinct colonies. The tubes were then transferred to a shaking incubator overnight to facilitate bacterial growth.

Plasmid DNA Isolation

Plasmid DNA was isolated using the QIAprep Spin Miniprep Kit (QIAGEN). A total of 1500 μL of bacterial DNA culture mix was transferred from the liquid culture tubes into 1.5 mL Eppendorf tubes. The tubes were centrifuged at 10,000 rcf for 5 minutes, and the resulting supernatant was discarded to remove unwanted cellular debris. The bacterial pellets were then resuspended in 250 μL of Buffer P1 and mixed thoroughly using a pipette to ensure uniform suspension. To lyse the bacterial cells, 250 μL of Buffer P2 was added to each tube, and the tubes were inverted 4–6 times to ensure even mixing. The lysis reaction was kept under 5 minutes to prevent DNA degradation. Once the solution became less cloudy, 350 μL of Buffer N3 was added to each tube, forming a precipitate, and the tubes were centrifuged at maximum speed for 10 minutes. Following centrifugation, 800 μL of supernatant was carefully transferred to QIAprep spin columns, avoiding the pellets. The columns were placed into collection tubes and centrifuged at 10,000 rcf for 1 minute. The flow-through, which contained unwanted bacterial components, was discarded in the designated chemical waste jar. To further purify the plasmid DNA and remove endotoxins, 500 μL of Buffer PB was added to each column, followed by centrifugation for 1 minute. Then, the flow-through was discarded again. This step was repeated using 750 μL of Buffer PE, followed by another centrifugation step. The spin columns were then centrifuged dry for 1 minute to remove any residual wash buffer. For elution, the spin

columns were transferred into fresh, labeled centrifuge tubes. 50 μL of water was added to each column, incubated for 1 minute, and centrifuged for another 1 minute. The final DNA sample was then sent for sequencing.

Lentiviral Transduction and Selection

Transfection Setup

A standard transfection protocol was developed for introducing plasmids into HeLa cells. Nine PCR tubes were labeled and arranged as follows:

- Four tubes designated for different transfection conditions (ex: mock, mCherry, Ted-Citrine, and co-transfection).
- One tube for Lipofectamine dilution.
- Four tubes for the final mixture of plasmids and Lipofectamine.

Plasmids were first diluted in OptiMEM, with 160 μL of OptiMEM added to each of the first four tubes. Separately, Lipofectamine was diluted by adding 640 μL of OptiMEM to the designated Lipofectamine dilution tube. Then, 38.4 μL of Lipofectamine was added and gently mixed. After dilution, the Lipofectamine and plasmid solutions were combined, with 150 μL of diluted Lipofectamine solution added to each empty mixing tube, followed by 150 μL of the corresponding plasmid solution, resulting in a total volume of 300 μL per tube. The mixtures were incubated at room temperature for 5 minutes, allowing the lipid-DNA complexes to form. After incubation, 250 μL of the transfection mixture was added dropwise to each well, ensuring

even distribution by gently swirling the plate. The plate was then returned to the incubator for 24 hours.

This transfection protocol was used for all direct plasmid transfections into HeLa cells, such as mCherry and Citrine constructs. For lentiviral production, lentiviral plasmids were transfected into HEK293T cells using the same protocol described above.

Lentiviral Infection and Selection

After 24–48 hours of transfection, the lentiviral supernatant was collected and filtered using a 0.45 µm syringe filter to remove cell debris. The virus-containing media was stored at 4°C for short-term use or -80°C for long-term use. HeLa cells were then infected with lentiviral supernatant with Polybrene (8 µg/mL) to enhance viral entry. After 24 hours, the virus-containing media was removed and replaced with fresh media. Cells were incubated for 48 hours. Afterwards, puromycin (2 µg/mL) was added for selection. Cells were maintained under selection for 5–7 days. This ensured that only successfully transduced cells expressing BIM or Citrine-DHFR remained.

Bleomycin Dose-Response

Bleomycin selection was performed to eliminate non-transduced cells and create a stable population of Citrine-expressing cells. To establish an effective selection concentration, a dose-response assay was conducted. HeLa WT and DKO cells were seeded in 24-well plates at a density of 25,000 cells per well and treated with a serial dilution of bleomycin to determine the minimum concentration required to eliminate all uninfected cells while allowing transduced cells to survive.

A bleomycin stock solution (20 $\mu\text{g}/\text{mL}$) was prepared and diluted 1:5000 in DMEM to generate the highest concentration. A series of four additional 2X dilutions were performed to create a dose range from 10 $\mu\text{g}/\text{mL}$ to 625 ng/mL , with a DMEM-only control well. Each well received 250 μL of 2X bleomycin solution, followed by 250 μL of a prepared cell suspension (100,000 cells/ mL), resulting in a final volume of 500 μL per well.

Cells were incubated under standard conditions. The effectiveness of bleomycin-mediated selection was assessed morphologically using light microscopy. The goal was to identify the lowest concentration that eliminated all uninfected cells while leaving transduced cells intact. Fluorescence microscopy was used to confirm Citrine expression in the surviving cell population. Flow cytometry was performed separately to verify the percentage of Citrine-positive cells in the fully selected population once uninfected cells had been eliminated.

Experimental Assays

Flow Cytometry Sample Preparation

After 24 hours of incubation, the 6-well plate was retrieved from the incubator, and the cells were examined under the microscope to assess their density and health. Cells were trypsinized, centrifuged, and resuspended in 250 μL HBSS. Before running the flow cytometry analysis, the samples were filtered into flow cytometry sample tubes with 35 μm mesh filter caps. The pipette tip was pressed against the mesh filter, and the resuspended cells were carefully pipetted through. Finally, each flow cytometry tube was labeled appropriately to match the experimental conditions.

Flow Cytometry Analysis

Laser channels were selected for fluorescence detection using an Attune NxT four laser flow cytometer. Next, plots were configured for analysis. The X-axis was set to Forward Scatter-Area to measure the size of a cell, and the Y-axis was set to Blue Laser 2 Channel for detection of Citrine fluorescence, with the excitation wavelength of the laser set at 488nm and detection between 570nm and 610nm, or Yellow Laser 2 Channel for detection of mCherry fluorescence, with the excitation wavelength at 561nm and detection between 613nm and 627nm. Four distinct plots were generated to visualize mCherry and Citrine fluorescence intensity, including a co-transfection plot to assess the correlation between the two fluorescent markers. Before running each sample, the tubes were vortexed to ensure a uniform cell suspension. The samples were then processed through the flow cytometer. The data was used to assess transfection efficiency and expression levels.

TMP Induction

The inducibility of Citrine-DHFR was assessed by treating cells with varying concentrations of trimethoprim (TMP) and monitoring fluorescence over time. A stock solution of 10 mM TMP was prepared in DMSO and diluted in culture media to final concentrations ranging from 0.1 to 10 μ M. One day after cell seeding, TMP-containing media was applied to cells for 24–48 hours, with control wells receiving equivalent volumes of DMSO.

Live-cell imaging was performed using the IncuCyte system, capturing time-lapse fluorescence measurements over the treatment period. This imaging step was conducted to track fluorescence changes qualitatively and ensure that cells remained viable throughout the

experiment. Quantification of TMP-mediated Citrine stabilization was performed using flow cytometry, rather than live-cell imaging. After the imaging phase, the same cells were harvested for flow cytometry analysis using the Citrine analysis parameters described above.

BH3 Profiling

The percentage of cytochrome c-negative cells was used as a quantitative measure of MOMP. Cells were treated with BH3 peptides at varying concentrations to assess mitochondrial apoptotic response. To permeabilize the plasma membrane and allow peptides to access the mitochondria, a 2X Membrane Extraction Buffer (MEB) with digitonin was prepared by adding 2uL of 1% digitonin per mL of MEB, yielding a digitonin concentration of 0.002% (2X), which was later mixed with an equal volume of cell suspension in MEB to give a 0.001% (1X) digitonin concentration after dilution. The 2X MEB mixture was then distributed into 8 tubes, each containing 100uL to which 2uL of the respective BH3 peptide concentration was added. The BH3 peptide stock solutions were also prepared as a 2X serial dilution, with final concentrations of 1 mM, 0.3 mM, 0.1 mM, 0.03 mM, 0.01 mM, 0.003 mM, 0.001 mM, and a DMSO control. Each well ultimately received 25 μ L of the peptide mixture in MEB. To ensure experimental reproducibility, the assay was performed with three replicate wells per condition.

For seeding, cells were retrieved from a culture flask and counted to determine the volume required for experimental conditions. The goal was to plate 10,000 cells per well, and calculations were adjusted based on the measured viable cell density. Cells were first centrifuged at 1,000 RPM for 5 minutes. After centrifugation, the supernatant was removed, ensuring the cell

pellet remained undisturbed. Cells were then resuspended in MEB, thoroughly mixed by pipetting, and transferred into a 5 mL tube for plating. Using a repeater pipette, 25 μ L of the resuspended cell solution was dispensed into each well of the prepared peptide plate. Plates were then incubated for 1 hour at 25°C. To halt the reaction and fix the cells, 15 μ L of 8% paraformaldehyde (PFA) was added to each well using a repeating pipette, followed by a 10-minute incubation at room temperature. To stop fixation, 35 μ L of N2 buffer, a HEPES (4-(2-hydroxyethyl) piperazine-1-ethanesulfonic acid) and sodium bicarbonate solution, was added to each well.

To assess mitochondrial apoptotic response, cells were stained with DAPI (4',6-diamidino-2-phenylindole) and an Alexa Fluor 647-conjugated cytochrome c antibody. The staining solution was prepared in a 5 mL tube by mixing: 2 mL of 10x intracellular staining buffer (ISB), 10 μ L of cytochrome c antibody, 20 μ L of DAPI. 10 μ L of stain was then added to each well, and plates were sealed and wrapped in foil to prevent light exposure. Stained plates were placed on a rocker in 4°C overnight to facilitate uniform staining. Analysis was conducted by flow cytometry to detect cytochrome c localization and DAPI staining, quantifying the percentage of cytochrome c-negative cells out of the total population of DAPI-positive cells. The results were indicative of MOMP and apoptotic response. The total well volume at the end of the assay was 110 μ L, composed of 25 μ L of cells, 25 μ L of peptides, 15 μ L of PFA, 35 μ L of N2 buffer, and 10 μ L of staining reagents. Data was analyzed by comparing variations in cytochrome c release across different peptide and compound concentrations.

III. Results

Plasmid Construct

To evaluate whether a TMP-inducible degron system could effectively control the intracellular delivery of pro-apoptotic peptides, I first designed and constructed the necessary plasmid templates. This involved engineering expression constructs that fused BH3 peptides or fluorescent reporters to a DHFR degron tag. SnapGene software was used to construct the final template design for the BIM Expression plasmid (Figure 3).

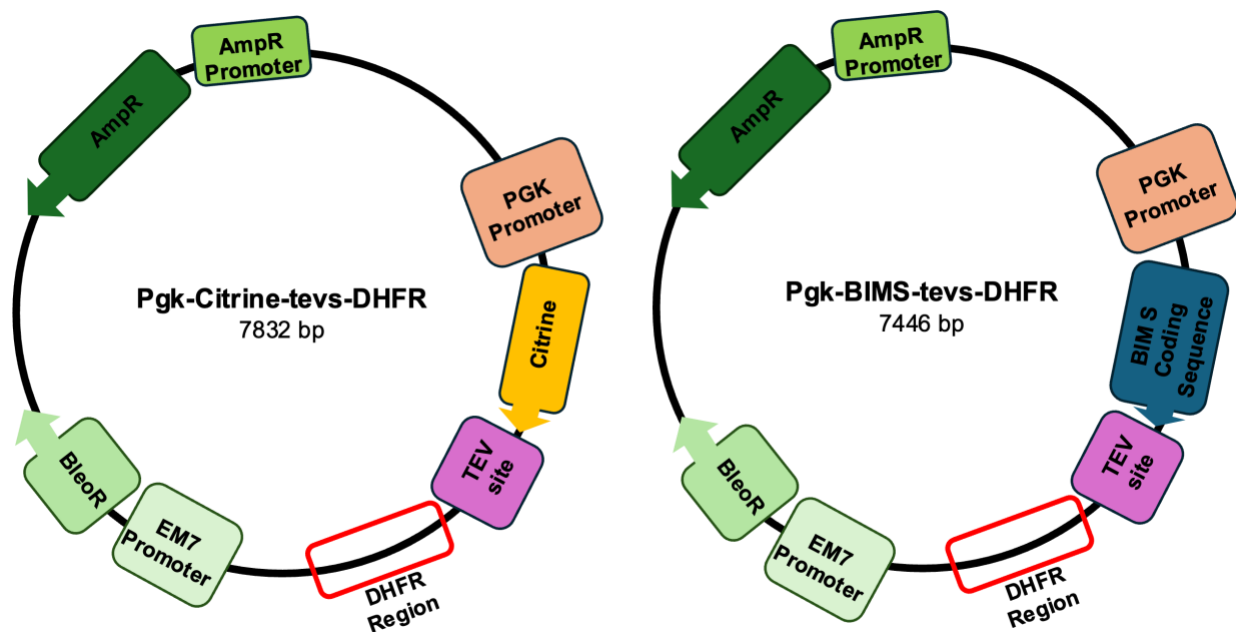


Figure 3: A simplified design of the Pkg-Citrine-tevs-DHFR template plasmid compared with the final Pkg-BIMS-tevs-DHFR plasmid. Key elements are included, such as the Citrine sequence replaced by the BIM S coding sequence, DHFR degradation domain, TEV cleavage

site, and selection markers (AmpR, BleoR). The construct is optimized for inducible apoptotic peptide expression.

Optimization of Transfection Efficiency

Comparison of Fluorescent Protein Expression in Transfection Experiments

Transfection efficiency was evaluated by measuring Citrine and mCherry expression in WT, DKO, BAX KO, and BAK KO HeLa cells. mCherry, like Citrine, is a fluorescent protein that was transfected in parallel via the PGK-H2BmCherry plasmid, with mCherry expression under the control of the constitutive PGK promoter. Flow cytometry analysis showed that mCherry expression was consistently higher than Citrine expression across all conditions, with the highest transfection efficiency observed in DKO cells (Figures 4,5). The gate parameters for Citrine positivity and mCherry positivity in the respective flow cytometry analyses was set based on the mock transfected WT cells. Thus, increased fluorescence over the mock transfection background was measured as either Citrine or mCherry positivity.

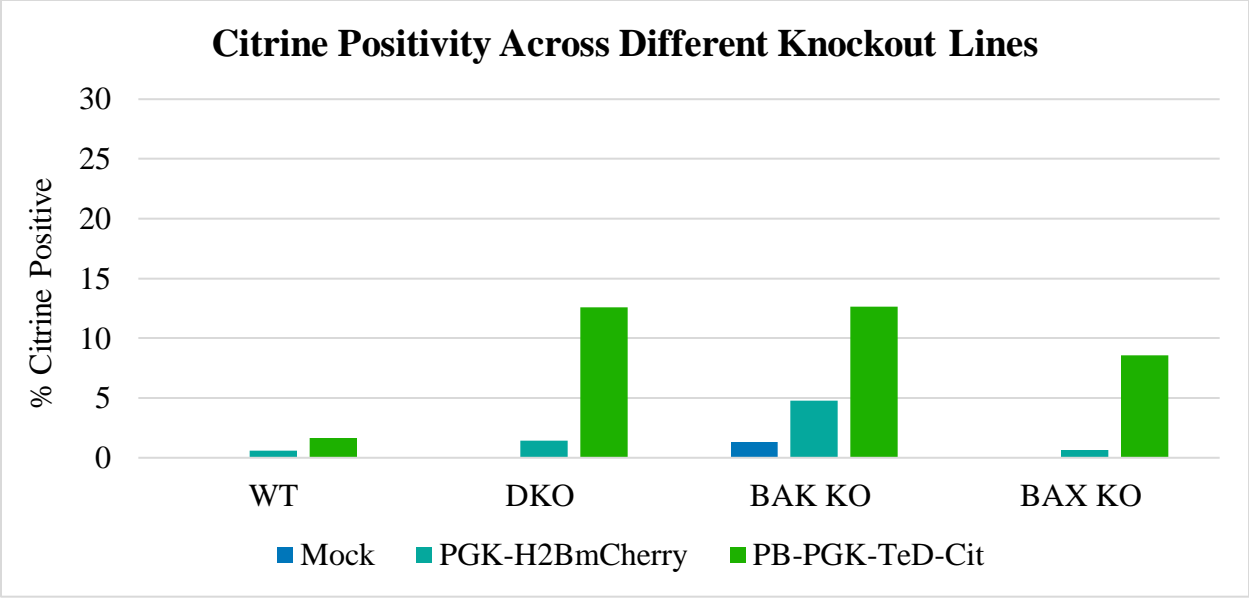


Figure 4: Citrine Positivity Across Different Knockout Lines after PB-PGK-TeD-Cit or

mCherry transfection. This bar graph represents the percentage of Citrine-positive cells gated from a transfection experiment. Wild type (WT), double knockout (DKO), BAX KO, and BAK KO HeLa cells were transfected with either a mock plasmid, mCherry, or Citrine constructs. DKO and BAK KO cells show the highest transfection efficiency with Citrine, while WT and BAX KO cells exhibit lower expression.

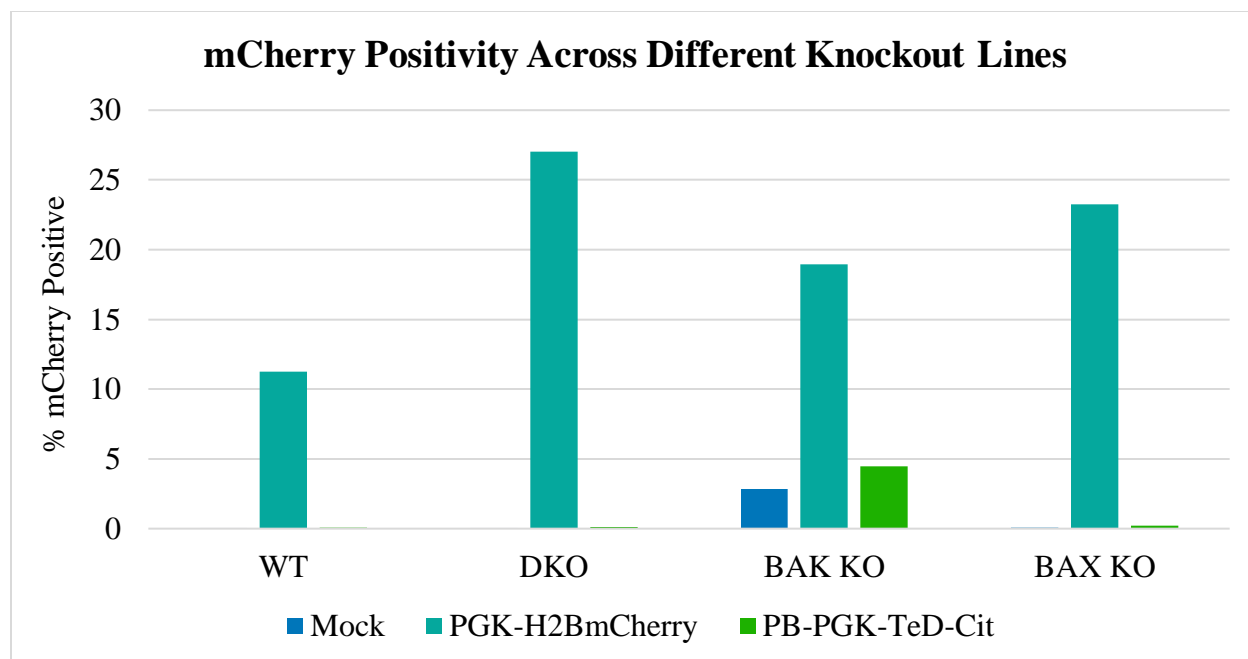


Figure 5: mCherry Positivity Across Different Knockout Lines after PB-PGK-TeD-Cit or mCherry transfection. This bar graph shows the percentage of mCherry-positive cells gated from the same transfection experiment as Figure 4 across different HeLa cell knockout lines. mCherry expression is higher than Citrine across all conditions, particularly in DKO and BAX KO cells, indicating different transfection efficiencies based on the fluorescent protein.

Transient Transfection Optimization

To optimize transfection efficiency while minimizing cytotoxicity, we first titrated Lipofectamine volumes across four HeLa cell lines: WT, BAX KO, BAK KO, and DKO. Lipofectamine-mediated transfection was optimized by titrating the volumes from 1.25 μ L to 5 μ L (Figure 6). The highest Citrine expression with minimal cytotoxicity was achieved using 5 μ L of Lipofectamine per 500 ng of plasmid DNA. Flow cytometry analysis at 24 hours post-

transfection showed that increasing Lipofectamine concentration correlated with an increase in Citrine fluorescence, though excessive Lipofectamine led to a decline in transfection efficiency in WT and BAK KO cells.

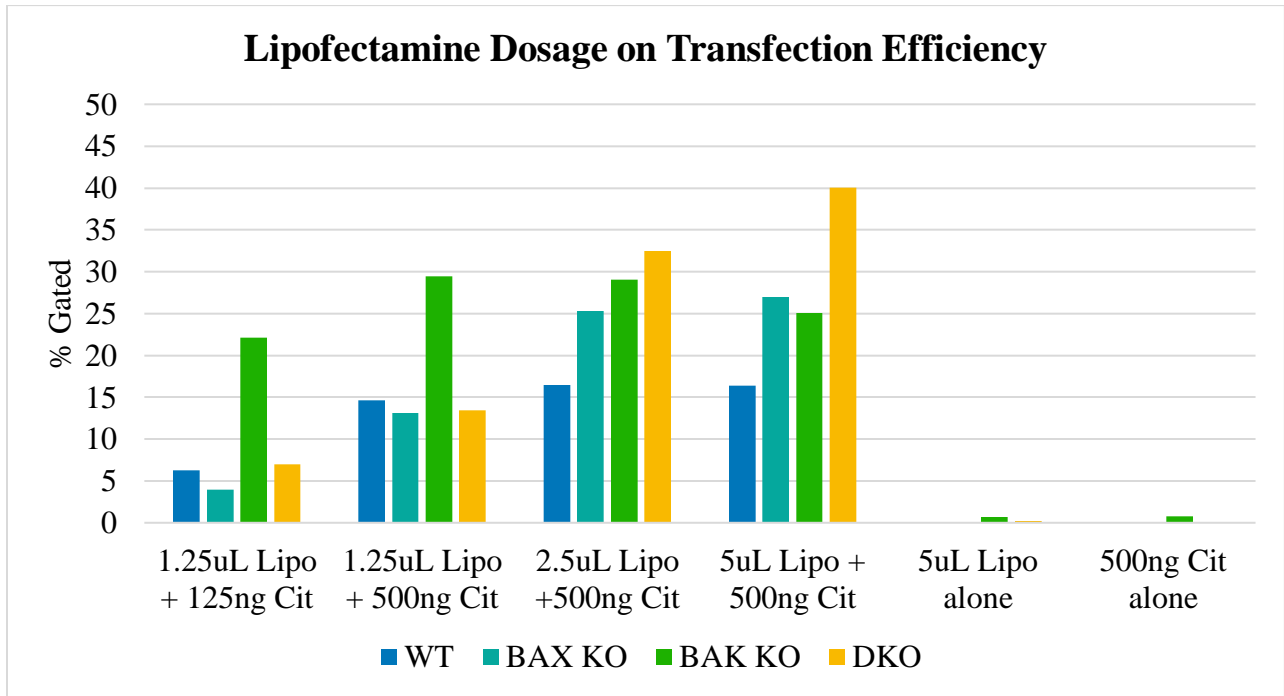


Figure 6: Percentage of Citrine-expressing Cells in Response to Lipofectamine Dosage. This figure illustrates transfection efficiency in WT, BAX KO, BAK KO, and DKO HeLa cells using varying amounts of Lipofectamine reagent. The optimal Lipofectamine dosage appears to be between 2.5 and 5 μ L, with DKO cells exhibiting the highest transfection efficiency.

Next, we tested the effect of plasmid DNA concentration on transfection efficiency by transfecting cells with 50 ng, 100 ng, and 200 ng of PB-PGK-Cit-TEVP-DHFR (Figure 7,8). We noted that the knockout HeLa lines, which are less sensitive to apoptosis, showed higher

apparent transfection efficiency. This could indicate that the Citrine plasmid (or the transfection conditions) could be inducing apoptotic cell death. Flow cytometry analysis at 24 and 48 hours post-transfection showed a dose-dependent increase in Citrine-positive cells between 50 ng and 100 ng. However, at the 48 hour mark, for most cell lines, Citrine expression plateaued or decreased at 200 ng (Figure 8). This suggests that while higher DNA concentrations promote transfection, they may also induce cytotoxicity. This effect was most apparent in WT and BAK KO cells, where the drop in Citrine positivity likely reflects transfection-induced apoptotic cell death.

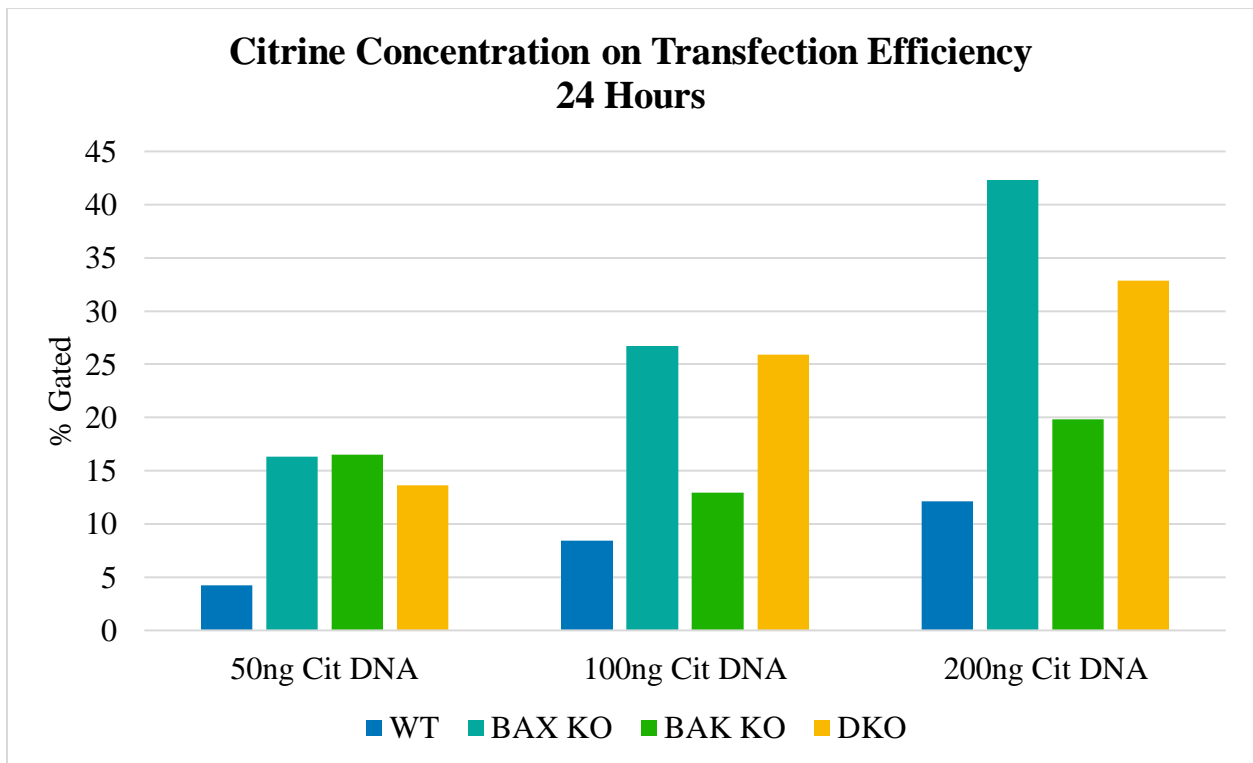


Figure 7: Citrine Expression at 24 Hours Post-Transfection. This figure presents flow cytometry data for Citrine expression at 24 hours post-transfection, comparing different DNA concentrations (50 ng, 100 ng, and 200 ng). Higher DNA concentrations generally lead to greater transfection efficiency, though differences are observed across cell lines.

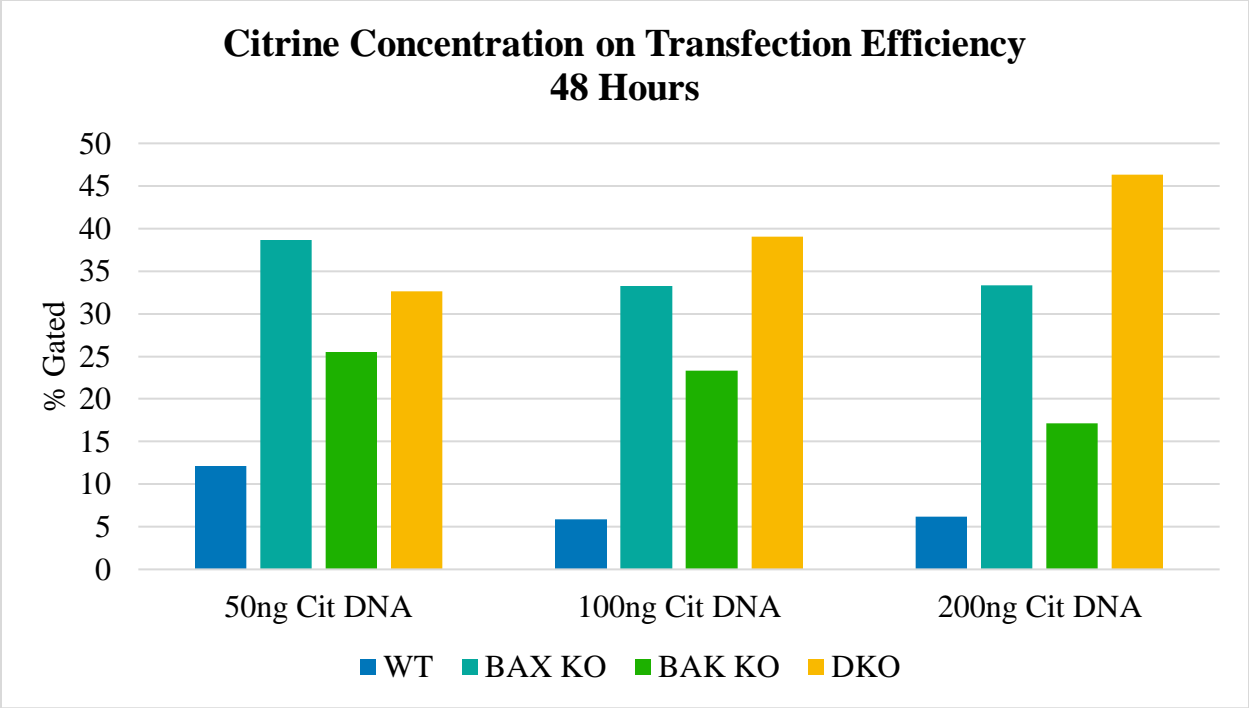


Figure 8: Citricine Expression at 48 Hours Post-Transfection. This figure displays the percentage of Citricine-positive cells at 48 hours post-transfection. Unlike the last time point, higher DNA concentrations generally lead to lower transfection efficiency, shown by the trends in WT, BAX KO, and BAK KO cell lines.

Apoptotic Peptide Expression with Trimethoprim

Dose-Dependent Citrine Expression

To assess whether the DHFR degradation system could be controlled with trimethoprim (TMP), Citrine expression was measured in response to increasing TMP concentrations. HeLa cells stably expressing the Citrine-DHFR construct were treated with TMP ranging from 625nM to 10uM, and flow cytometry analysis was performed 48 hours post-treatment. The pLX_TRC311_Citrine-tevs-DHFR plasmid was first generated by Gateway cloning, followed by lentiviral packaging and infection of HeLa cells. After infection, cells were selected with puromycin, ensuring stable integration of the Citrine-DHFR fusion protein before TMP treatment. Citrine fluorescence was observed at all tested TMP conditions, with expression levels remaining relatively consistent across the dose range (Figure 9,10). This indicates that TMP-mediated stabilization of the DHF fusion protein is highly efficient, with expression levels reaching a plateau at 625nM. However, a minimum effective TMP dose for DHFR fusion construct induction has not yet been determined. A follow-up experiment would be to test TMP concentrations below 625nM to identify the lowest dose capable of stabilizing the DHFR fusion protein.

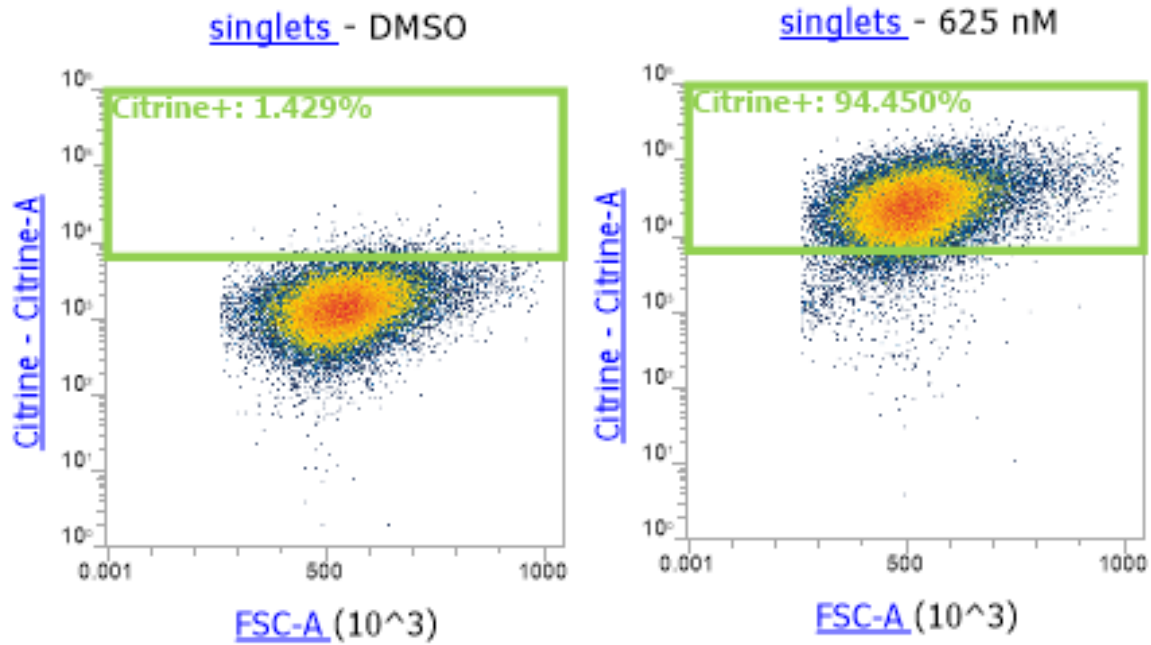


Figure 9: Flow cytometry scatter plots displaying the percentage of Citrine-positive cells after TMP treatment. DMSO control is compared with 625 nM TMP treatment conditions. TMP induces a substantial increase in Citrine expression (from 1.429% to 94.450%), confirming DHFR stabilization.

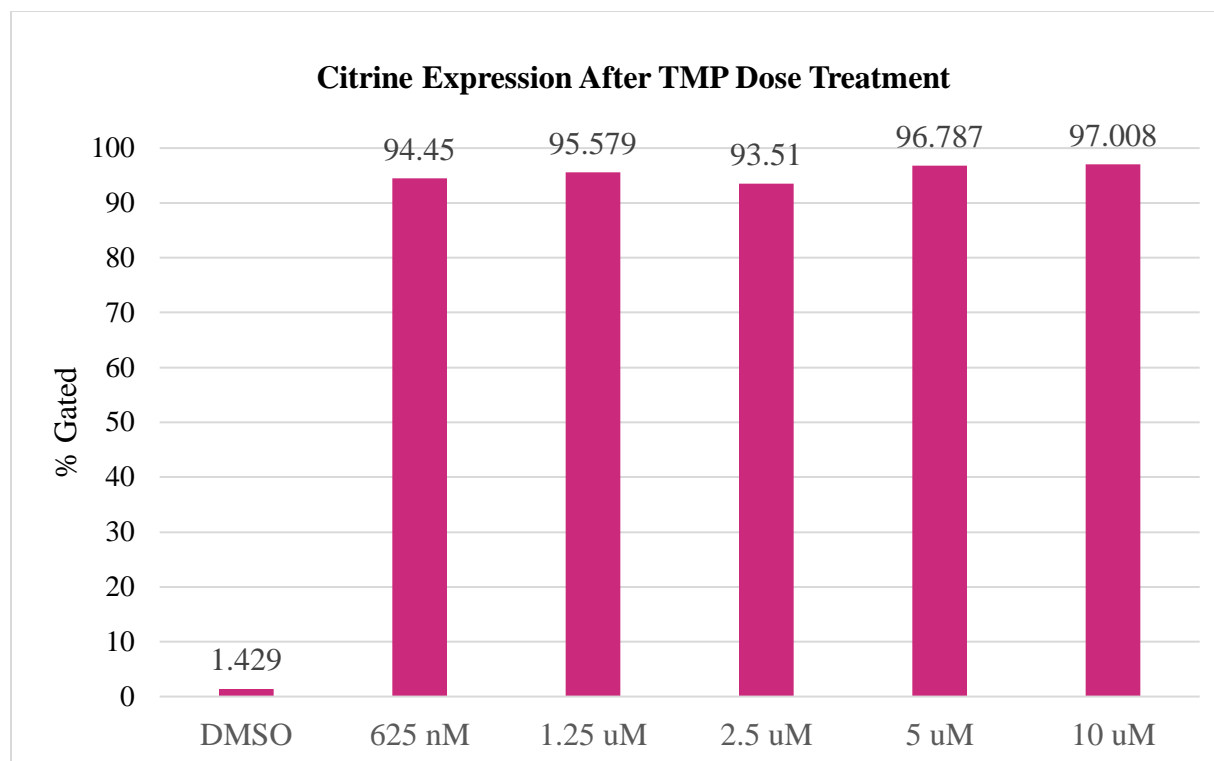


Figure 10: Citrine Expression 48 Hours After TMP Treatment. This graph displays the percentage of Citrine-positive cells following TMP treatment at increasing concentrations (625 nM to 10 μ M). The results were obtained via flow cytometry and demonstrate TMP-mediated stabilization of the DHFR-Citrine construct.

Importantly, untreated cells exhibited only 1.429% Citrine-positive expression, indicating that background leaky expression of the construct was minimal. However, as a small proportion of untreated cells displayed detectable fluorescence, some level of basal DHFR stabilization may occur in the absence of TMP.

Kinetic Analysis of Apoptotic Induction

TMP Induction System

To investigate the kinetics of TMP-induced apoptosis, fluorescence microscopy and flow cytometry were used to monitor Citrine expression and cytochrome c release at various time points following TMP treatment (Figure 11).

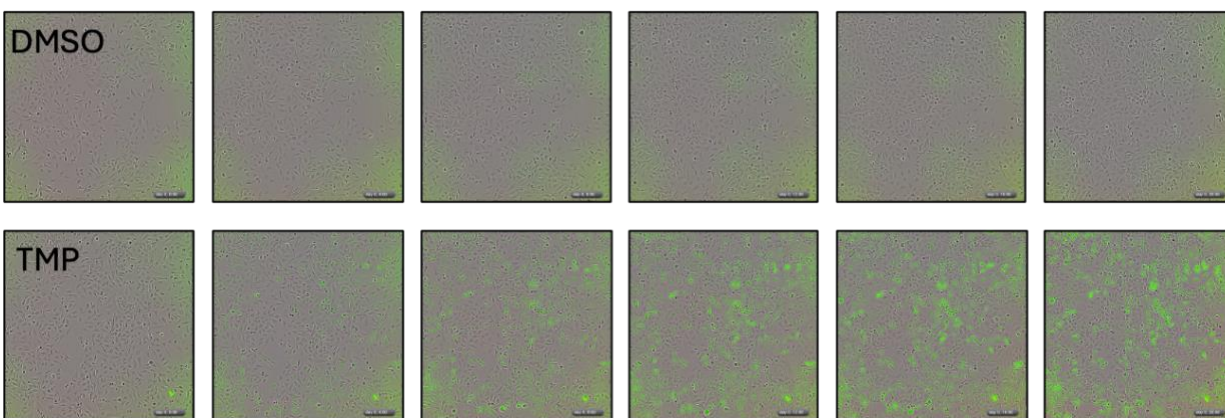


Figure 11: TMP Response Displaying Citrine Expression at 0 Hours to 20 hours.

Fluorescence microscopy images show Citrine expression in HeLa cells treated with DMSO (top row) or 625 nM TMP (bottom row) at hour 0, hour 4, hour 8, hour 12, hour 16, and hour 20 (from left to right). No significant Citrine fluorescence is observed at 0 hours. However, at the 20 hour mark, cells treated with 625 nM TMP exhibit strong Citrine fluorescence compared to the DMSO control.

IV. Discussion

For our key findings, we evaluated transfection efficiency across multiple HeLa knockout lines. We found that cells with impaired apoptotic machinery, particularly double knockouts, exhibited higher expression levels. This likely reflects increased resistance to transfection-induced cell stress. These findings inform both the choice of the cell lines optimal for future experiments and suggest that baseline apoptotic sensitivity may also influence the success of BH3 peptide delivery. Additionally, we were able to optimize key transfection parameters, including DNA amount and lipofectamine dosage, to balance expression of the DNA with cell viability. In parallel, transitioning to a lentivirus-mediated system, we successfully established a stable HeLa cell line expressing a Citrine-DHFR fusion construct. Using this system, we demonstrated the protein expression could be tightly regulated through TMP treatment. We observed a clear trend in response to TMP dose, which allows us to refine the timing and concentration necessary for effective induction. Although we did observe a small amount of leaky expression in cells that were not treated, the contrast with TMP-treated conditions was substantial. These results supported the robust DHFR degon system.

This work lays the foundation for the application of the TMP-inducible platform to efficiently deliver BH3 peptide for apoptosis quantification. Ongoing experiments will further pinpoint the optimal induction conditions for other constructs, including BIM-DHFR, and determine whether this system can reliably trigger apoptosis in primed cells.

My thesis focused on developing a novel approach to measure apoptotic priming without the need for plasma membrane permeabilization by building upon existing tools in the field of synthetic biology and bioengineering. These methods, such as the DHFR degon system, were

adapted and extended to deliver pro-apoptotic peptides in a controllable, intracellular manner. Rather than relying on endogenously expressed proteins, this strategy employs externally introduced, engineered constructs to modulate apoptotic signaling. The results demonstrate that TMP-mediated stabilization of the Citrine-DHFR fusion protein effectively induces fluorescence, confirming that the degon system functions as expected. This validation of the TMP-inducible system is a critical first step toward our goal of using an oligonucleotide-based method to deliver pro-apoptotic peptides for BH3 profiling. While we have successfully completed and design and generated the necessary plasmids in silico and initiated experimental validation, additional steps using site directed mutagenesis and Golden Gate cloning are ongoing.

Compared to traditional BH3 profiling, our approach aims to offer a more physiologically relevant method to assess apoptotic priming by avoiding the unintended stress responses caused by membrane permeabilization. However, as our system transitions from a fluorescent protein-based system to a BH3 peptide-based system, further optimization is needed to confirm that pro-apoptotic peptides expressed through the system recapitulate the effects of direct peptide delivery. The main strength of our approach is its potential for greater experimental flexibility and compatibility with live cell analysis, which is difficult with traditional BH3 profiling methods. However, at this stage, there are limitations. Most importantly, while our plasmid construct has been successful in inducible fluorescent protein expression, we have not yet assessed whether the system can efficiently trigger apoptosis once the BH3 peptides are introduced, which would be our highest priority next step. After generating the BH3-DHFR peptide fusion plasmids, the next step is comparing this method to direct peptide delivery. Before fully integrating this method into BH3 profiling systems, experimental comparison will be essential to validate our system against established methods and ensure that the kinetics of

peptide expression align with those observed in these existing methods. Furthermore, through an assessment of apoptotic sensitivity in multiple cell models, we can determine whether our method provides a reliable read of apoptotic priming in various cell lines, particularly in cancer cell lines.

This research aligns closely with recent advancements in synthetic biology and cell engineering. The ability to precisely control apoptotic signaling through inducible oligonucleotide-mediated delivery systems fits within the growing efforts to engineer cellular systems with programmable responses. One recent example, Xia et al. (2024) developed “synoptosis” circuits that use synthetic proteolytic modules to direct cell death with user input, demonstrating the power of programmable protein circuits to actively dictate cell fate [32]. Beyond its immediate application in bioengineering research, our oligonucleotide-based approach to BH3 profiling has significant potential implications across multiple fields.

As mentioned, one major advantage of this method is its ability to assess apoptotic priming in intact cells without the need for membrane disruption. Traditional BH3 profiling methods require permeabilizing the plasma membrane to deliver synthetic peptides, which can introduce cellular stress and complicate downstream analyses such as RNA sequencing. Our approach preserves the cellular environment, allowing for more accurate and physiologically relevant apoptotic assessments while also enabling integration with single-cell analyses. As our system performs BH3 peptide delivery in living cells, those that do not undergo MOMP—unprimed cells—retain an intact membrane and remain viable. This allows for their continued culture and further downstream analysis. In contrast, traditional BH3 profiling involves permeabilization, which comprises membrane integrity even in unprimed cells. This prevents

their viability for future experiments. Our system, therefore, opens the possibility of prospectively identifying and studying the molecular features and survival mechanisms of unprimed cells that are able to resist apoptosis.

More broadly, in cancer research and therapy development, BH3 profiling has been instrumental in understanding how cancer cells can evade apoptosis. This has led to cancer therapies like the BCL-2 inhibitor Venetoclax. Our method could provide a more scalable and cost-effective approach to identifying specific processes in apoptotic pathways relevant to tumor development, which can aid in personalized cancer treatments. Similarly, drug screening can benefit from this approach, as traditional BH3 profiling relies on synthetic peptide delivery, which is costly and difficult to scale for large drug screens. Once our approach is validated, our platform could enable a more efficient screening procedure of novel pro-apoptotic compounds, including those designed through Golden Gate cloning. In future applications, these libraries of BH3 variants could soon incorporate peptide design predicted by machine learning models. For example, Bryant et al. (2021) demonstrated that machine learning enabled the design of highly functional and diverse protein variants by iteratively selecting and testing related sequences [33]. Similar strategies can be used to predict and experimentally validate BH3 peptides, combining computational design with flexible cloning. By uniting these approaches, this system has the potential to accelerate therapeutic discovery while expanding the reach of apoptotic research.

While our study is still in progress, we have successfully taken important steps in validating a novel oligonucleotide-based approach to BH3 profiling. Our confirmation that the TMP-inducible Citrine-DHFR system functions as expected is a key milestone. Additionally, the successful completion of in-silico plasmid design and construction was a crucial step in

engineering this system, allowing functional validation before further experimental implementation. This approach efficiently streamlined the cloning process so that BH3 peptide integration could readily proceed. Further refinements and optimization steps will hopefully establish this novel approach as a robust tool for both research and clinical applications, expanding its reliability, scalability, and applicability in apoptotic studies and therapeutic development.

V. References

- [1] “Apoptosis (article) | Developmental biology,” Khan Academy. Accessed: Oct. 23, 2024. [Online]. Available: <https://www.khanacademy.org/science/biology/developmental-biology/apoptosis-in-development/a/apoptosis>
- [2] J. Yuan and B. A. Yankner, “Apoptosis in the nervous system,” *Nature*, vol. 407, no. 6805, pp. 802–809, Oct. 2000, doi: 10.1038/35037739.
- [3] M. E. Guicciardi, H. Malhi, J. L. Mott, and G. J. Gores, “Apoptosis and Necrosis in the Liver,” *Compr. Physiol.*, vol. 3, no. 2, p. 10.1002/cphy.c120020, Apr. 2013, doi: 10.1002/cphy.c120020.
- [4] Y. Teraki and T. Shiohara, “Apoptosis and the skin,” *Eur. J. Dermatol. EJD*, vol. 9, no. 5, pp. 413–425; quiz 426, 1999.
- [5] A. Ramachandran, M. Madesh, and K. A. Balasubramanian, “Apoptosis in the intestinal epithelium: its relevance in normal and pathophysiological conditions,” *J. Gastroenterol. Hepatol.*, vol. 15, no. 2, pp. 109–120, Feb. 2000, doi: 10.1046/j.1440-1746.2000.02059.x.
- [6] P. G. Ekert and D. L. Vaux, “Apoptosis and the immune system,” *Br. Med. Bull.*, vol. 53, no. 3, pp. 591–603, 1997, doi: 10.1093/oxfordjournals.bmb.a011632.
- [7] D. Plesca, S. Mazumder, and A. Almasan, “DNA Damage Response and Apoptosis,” *Methods Enzymol.*, vol. 446, p. 107, 2008, doi: 10.1016/S0076-6879(08)01606-6.
- [8] B. J. Thomson, “Viruses and apoptosis,” *Int. J. Exp. Pathol.*, vol. 82, no. 2, p. 65, Apr. 2001, doi: 10.1111/j.1365-2613.2001.iep0082-0065-x.
- [9] T. J. McDonnell *et al.*, “*bcl-2*-Immunoglobulin transgenic mice demonstrate extended B cell survival and follicular lymphoproliferation,” *Cell*, vol. 57, no. 1, pp. 79–88, Apr. 1989, doi: 10.1016/0092-8674(89)90174-8.

- [10] S. LI *et al.*, “XIAP expression is associated with pancreatic carcinoma outcome,” *Mol. Clin. Oncol.*, vol. 1, no. 2, pp. 305–308, 2013, doi: 10.3892/mco.2013.58.
- [11] R. Halaby, “Apoptosis and Autoimmune Disorders,” in *Autoimmune Diseases - Contributing Factors, Specific Cases of Autoimmune Diseases, and Stem Cell and Other Therapies*, IntechOpen, 2012. doi: 10.5772/48164.
- [12] A. C. Doran, A. Yurdagul, and I. Tabas, “Efferocytosis in health and disease,” *Nat. Rev. Immunol.*, vol. 20, no. 4, pp. 254–267, Apr. 2020, doi: 10.1038/s41577-019-0240-6.
- [13] R. Kumar, P. E. Herbert, and A. N. Warrens, “An introduction to death receptors in apoptosis,” *Int. J. Surg.*, vol. 3, no. 4, pp. 268–277, Jan. 2005, doi: 10.1016/j.ijssu.2005.05.002.
- [14] “Intrinsic and Extrinsic Pathways of Apoptosis - US.” Accessed: Oct. 26, 2024. [Online]. Available: <https://www.thermofisher.com/us/en/home/life-science/antibodies/antibodies-learning-center/antibodies-resource-library/cell-signaling-pathways/cellular-apoptosis-pathway.html>
- [15] A. Yanumula and J. K. Cusick, “Biochemistry, Extrinsic Pathway of Apoptosis,” in *StatPearls*, Treasure Island (FL): StatPearls Publishing, 2024. Accessed: Oct. 26, 2024. [Online]. Available: <http://www.ncbi.nlm.nih.gov/books/NBK560811/>
- [16] J. Kale, E. J. Osterlund, and D. W. Andrews, “BCL-2 family proteins: changing partners in the dance towards death,” *Cell Death Differ.*, vol. 25, no. 1, pp. 65–80, Jan. 2018, doi: 10.1038/cdd.2017.186.
- [17] V. D. G. Moore and A. Letai, “BH3 profiling – measuring integrated function of the mitochondrial apoptotic pathway to predict cell fate decisions,” *Cancer Lett.*, vol. 332, no. 2, p. 202, Jan. 2012, doi: 10.1016/j.canlet.2011.12.021.

- [18] S. Elmore, “Apoptosis: A Review of Programmed Cell Death,” *Toxicol. Pathol.*, vol. 35, no. 4, p. 495, 2007, doi: 10.1080/01926230701320337.
- [19] L. Lindenboim, H. Zohar, H. J. Worman, and R. Stein, “The nuclear envelope: target and mediator of the apoptotic process,” *Cell Death Discov.*, vol. 6, no. 1, pp. 1–11, Apr. 2020, doi: 10.1038/s41420-020-0256-5.
- [20] M. Battistelli and E. Falcieri, “Apoptotic Bodies: Particular Extracellular Vesicles Involved in Intercellular Communication,” *Biology*, vol. 9, no. 1, p. 21, Jan. 2020, doi: 10.3390/biology9010021.
- [21] J. C. Mills, N. L. Stone, and R. N. Pittman, “Extranuclear Apoptosis: The Role of the Cytoplasm in the Execution Phase,” *J. Cell Biol.*, vol. 146, no. 4, p. 703, Aug. 1999, doi: 10.1083/jcb.146.4.703.
- [22] C. Fraser, J. Ryan, and K. Sarosiek, “BH3 profiling: a functional assay to measure apoptotic priming and dependencies,” *Methods Mol. Biol. Clifton NJ*, vol. 1877, p. 61, 2019, doi: 10.1007/978-1-4939-8861-7_4.
- [23] D. S. Potter, R. Du, P. Bholra, R. Bueno, and A. Letai, “Dynamic BH3 profiling identifies active BH3 mimetic combinations in non-small cell lung cancer,” *Cell Death Dis.*, vol. 12, no. 8, pp. 1–12, Jul. 2021, doi: 10.1038/s41419-021-04029-4.
- [24] K. A. Sarosiek, T. N. Chonghaile, and A. Letai, “Mitochondria: gatekeepers of response to chemotherapy,” *Trends Cell Biol.*, vol. 23, no. 12, p. 10.1016/j.tcb.2013.08.003, Dec. 2013, doi: 10.1016/j.tcb.2013.08.003.
- [25] A. W. Roberts, S. Stilgenbauer, J. F. Seymour, and D. C. S. Huang, “Venetoclax in Patients with Previously Treated Chronic Lymphocytic Leukemia,” *Clin. Cancer Res.*, vol. 23, no. 16, pp. 4527–4533, Aug. 2017, doi: 10.1158/1078-0432.CCR-16-0955.

- [26] M. A. Anderson *et al.*, “The BCL2 selective inhibitor venetoclax induces rapid onset apoptosis of CLL cells in patients via a TP53-independent mechanism,” *Blood*, vol. 127, no. 25, p. 3215, Apr. 2016, doi: 10.1182/blood-2016-01-688796.
- [27] X. J. Gao, L. S. Chong, M. S. Kim, and M. B. Elowitz, “Programmable protein circuits in living cells,” *Science*, vol. 361, no. 6408, p. 1252, Sep. 2018, doi: 10.1126/science.aat5062.
- [28] H.-C. Tai and E. M. Schuman, “Ubiquitin, the proteasome and protein degradation in neuronal function and dysfunction,” *Nat. Rev. Neurosci.*, vol. 9, no. 11, pp. 826–838, Nov. 2008, doi: 10.1038/nrn2499.
- [29] M. Iwamoto, T. Björklund, C. Lundberg, D. Kirik, and T. J. Wandless, “A General Chemical Method to Regulate Protein Stability in the Mammalian Central Nervous System,” *Chem. Biol.*, vol. 17, no. 9, pp. 981–988, Sep. 2010, doi: 10.1016/j.chembiol.2010.07.009.
- [30] M. Gossen, S. Freundlieb, G. Bender, G. Müller, W. Hillen, and H. Bujard, “Transcriptional Activation by Tetracyclines in Mammalian Cells,” *Science*, vol. 268, no. 5218, pp. 1766–1769, Jun. 1995, doi: 10.1126/science.7792603.
- [31] R. Pan, J. Ryan, D. Pan, K. W. Wucherpfennig, and A. Letai, “Augmenting NK cell-based immunotherapy by targeting mitochondrial apoptosis,” *Cell*, vol. 185, no. 9, pp. 1521–1538.e18, Apr. 2022, doi: 10.1016/j.cell.2022.03.030.
- [32] S. Xia *et al.*, “Synthetic protein circuits for programmable control of mammalian cell death,” *Cell*, vol. 187, no. 11, pp. 2785–2800.e16, May 2024, doi: 10.1016/j.cell.2024.03.031.
- [33] D. H. Bryant *et al.*, “Deep diversification of an AAV capsid protein by machine learning,” *Nat. Biotechnol.*, vol. 39, no. 6, pp. 691–696, Jun. 2021, doi: 10.1038/s41587-020-00793-4.